

NASA Contractor Report 3816



Advanced Composite Vertical Fin for L-1011 Aircraft

*Design, Manufacture, and Test
(Executive Summary)*

A. C. Jackson

CONTRACT NAS1-14000
SEPTEMBER 1984

Date for general
release will be three (3) years from date indicated on
the document.

NASA

NASA Contractor Report 3816

Advanced Composite Vertical Fin for L-1011 Aircraft

*Design, Manufacture, and Test
(Executive Summary)*

A. C. Jackson
*Lockheed-California Company
Burbank, California*

Prepared for
Langley Research Center
under Contract NAS1-14000



National Aeronautics
and Space Administration

Scientific and Technical
Information Branch

1984

FOREWORD

This report was prepared by the Lockheed-California Company, Lockheed Corporation, Burbank, California, under contract NAS1-14000 and it is the executive summary report for the advanced composite vertical fin program. The program is sponsored by the National Aeronautics and Space Administration (NASA), Langley Research Center.

The program managers for Lockheed were Mr. Fred C. English and Mr. W. F. Priest. Mr. Herman L. Bohon was project manager for NASA Langley. The technical representatives for NASA Langley were Dr. Herbert A. Leybold and Mr. Marvin B. Dow.

Engineering, Manufacturing and Quality Assurance personnel from Lockheed-California Company, and Lockheed-Georgia Company were involved in the program.

TABLE OF CONTENTS

<u>Section</u>	<u>Page</u>
FOREWORD	iii
LIST OF ILLUSTRATIONS	vii
LIST OF TABLES	ix
SUMMARY.	1
INTRODUCTION	2
ADVANCED COMPOSITE VERTICAL FIN DESIGN	5
General Description	5
Design Criteria	5
Detail Design	6
Design Analysis	7
PRODUCIBILITY STUDY.	8
PROCESS VERIFICATION	11
ANCILLARY TEST PROGRAM	12
Material Verification	12
Concept Verification	14
PRODUCTION READINESS VERIFICATION TESTING	14
Fabrication	14
Static Tests	19
Durability Tests	21
FIN FABRICATION	24
Tooling	24
DETAIL FABRICATION	26
Covers	26
Spars	28
Ribs	29
ASSEMBLY	29
Subassembly of Spars	29
Assembly of Fin Box	29
QUALITY ASSURANCE	32

TABLE OF CONTENTS (Continued)

<u>Section</u>	<u>Page</u>
MANUFACTURING COST ANALYSIS	34
Final Cost Analysis	35
FULL-SCALE GROUND TESTS	36
Ground Test Setup and Loads	36
Ground test article No. 1 - Test History	38
Ground test article No. 1 - Failure Analysis	38
Ground test article No. 2	41
Static test	43
Damage Tolerance Testing	43
Discrete Damage Test and Repair	46
Residual Static Strength Test	46
Lessons Learned	49
CONCLUSIONS	50
REFERENCES	51

LIST OF ILLUSTRATIONS

<u>Figure</u>		<u>Page</u>
1	Master schedule for restructured program	3
2	Advanced composite vertical fin design configuration	6
3	ACVF skin ply buildup	6
4	Rib cap evolution	9
5	Solid web rib evolution	9
6	Design changes, spar web material change.	11
7	Spar web access hole	11
8	Spar web stiffener	12
9	Design allowables approach	13
10	T300/5208 unidirectional tape tensile strength design allowables	13
11	Typical cover specimen	18
12	Typical spar specimen	18
13	Cover static test results	20
14	Spar static test results.	20
15	Schematic of loads/thermal cycle for PRVT	22
16	Six covers in an environmental chamber	23
17	Six spars in an environmental chamber	23
18	Residual strength tests on PRVT covers.	25
19	Residual strength tests on PRVT spars	25
20	Diagram of composite spar molding fixture	26
21	Typical hat/skin assembly cure stacking arrangement	27
22	Loading stiffeners in front spar tool	28
23	Solid web bleeder stacking arrangement	30
24	Actuator and truss rib bleeder stacking arrangement	30
25	Installation of rear spar	31
26	Shipment of fin box on specially designed, shock-mounted dolly	32
27	Test installation of fin in load reaction frame	37
28	Test bending moment compared with design bending moment	37

LIST OF ILLUSTRATIONS (Continued)

<u>Figure</u>		<u>Page</u>
29	Photomicrograph of section from GTA front spar cap, right side at VSS 278.3	40
30	Schematic of original spar cap and redesigned spar cap	40
31	Spar cap reinforcement	42
32	Front spar to rib attachment reinforcement	42
33	Cover reinforcement	42
34	Impact damage locations	44
35	Location No. 2 damage growth	45
36	Simulated lightning damage	47
37	Damage repair	47
38	Fin box at the moment of failure	48
39	Shear rosette strain gage plots on tension cover in bay below the failure bay	48

LIST OF TABLES

<u>Table</u>		<u>Page</u>
I	CONCEPT VERIFICATION TEST RESULTS	15
II	COEFFICIENT OF VARIATION IN STATIC STRENGTH OF SOME STRUCTURAL MATERIALS	21
III	CAUSES FOR REJECTION OF RIB AND COVERS	33
IV	COST COMPARISON - SUMMARY	35
V	COST COMPARISON BY COMPONENT (CUMULATIVE AVERAGE - 100 UNITS)	35
VI	COMPARISON OF METAL FIN TO COMPOSITE FIN	41

ADVANCED COMPOSITE VERTICAL FIN FOR L-1011 AIRCRAFT -
DESIGN, MANUFACTURE AND TEST (EXECUTIVE SUMMARY)

EXECUTIVE SUMMARY

A. C. Jackson

SUMMARY

This report summarizes the engineering and manufacturing development activities of an advanced composite vertical fin for the L-1011 commercial transport aircraft. This program was divided into five phases:

Phase I (reference 1) consisted of preliminary design trade-off studies, material screening, and selection of the composite material system to be used. Also plans were prepared for the ancillary test program, quality control, and structural integrity control.

Phase II (reference 2) concentrated on the design and analysis of the full-scale box; the material testing for design allowables; producibility studies to identify the most cost effective fabrication techniques; process development and concept verification subcomponent testing.

Phase III (reference 3) consisted of static testing of 10 identical cover and 10 identical spar components to determine the range of production qualities and static strength variability. In addition, 12 more cover and 12 more spar components underwent long-term durability testing.

Phase IV (reference 4) consisted of the tool development; cover, spar and rib fabrication; and fin box assembly.

Phase V (reference 5) consisted of full-scale static, damage growth, and fail-safe tests.

The composite fin is a two-spar, multirib design with stiffened cocured graphite/epoxy tape covers and spars, and ribs consisting of graphite/epoxy tape caps with aluminum truss members or graphite/epoxy tape webs with syntactic core.

The structural analyses conducted on the composite fin in combination with materials testing, concept verification testing, and Production Readiness Verification Testing (Phase III) have verified the structural integrity of the design concepts and the analysis methods used in the design. Final substantiation was obtained by static, damage growth, and fail-safe tests conducted on two full-scale components.

Component manufacturing provided the necessary technical data to develop manufacturing cost analysis and material production cost projections. Production quality tooling was developed and components were fabricated in a production environment to produce flight quality hardware.

INTRODUCTION

The broad objective of the Aircraft Energy Efficiency (ACEE) Composite Structures Program is to accelerate the use of composite structures in new aircraft by developing technology and processes for early progressive introduction of composite structures into production commercial transport aircraft. This program, as one of several which are collectively aimed toward accomplishing that objective, has the specific objective to develop and manufacture advanced composite vertical fins for L-1011 transport aircraft. Laboratory tests and analyses have been made to substantiate that the composite fin can operate safely and economically under service loads and environments and will meet Federal Aviation Administration (FAA) requirements for installation on commercial aircraft. A limited quantity of units were fabricated to establish manufacturing methods and costs. The Advanced Composite Vertical Fin (ACVF) consists of over 76 percent advanced composite materials and weighs about 27 percent less than the metal fin it replaces.

The ACVF developed under this program consists of the entire main box structure of the vertical stabilizer for the L-1011 transport aircraft. The box structure extends from the fuselage production joint to the tip rib and includes the front and rear spars. It is 25 feet tall with a root box chord of 9 feet and represents an area of 150 square feet.

The primary objective of this program was to gain a high level of confidence in the structural integrity and durability of advanced composite primary structures. An important secondary objective was to gain sufficient knowledge and experience in manufacturing aircraft structures of advanced composite materials to assess properly their cost effectiveness.

The duration of this program was 102 months. The master schedule is shown in figure 1. The program was organized in five phases: Phase I, Engineering Development; Phase II, Design and Analysis; Phase III, Production Readiness Verification Tests (PRVT); Phase IV, Manufacturing Development; and Phase V, Ground Tests.

The Lockheed-California Company teamed with the Lockheed-Georgia Company in the development of the ACVF. Lockheed-California Company, as prime contractor, had overall program responsibility and designed and fabricated the covers and the ribs, conducted the full-scale ground tests, and the PRVT program. Lockheed-Georgia Company designed and fabricated the front, rear, and auxiliary spars, and assembled the composite fin at Lockheed's plant in Meridian, Mississippi, where the metallic L-1011 vertical fins were assembled.

During the initial phases of this program, several tasks were accomplished: the conceptual development was completed; an ancillary test program was initiated to examine the behavior of the composite material in various environments; a 260 F cure material, T300/5209, was selected as the result of screening tests; detail design, using the selected material, was completed; the design and fabrication of a tape-laying tool for manufacturing covers was completed; and some of the full-scale tools for fabrication of covers, spars, and ribs were completed and proven.

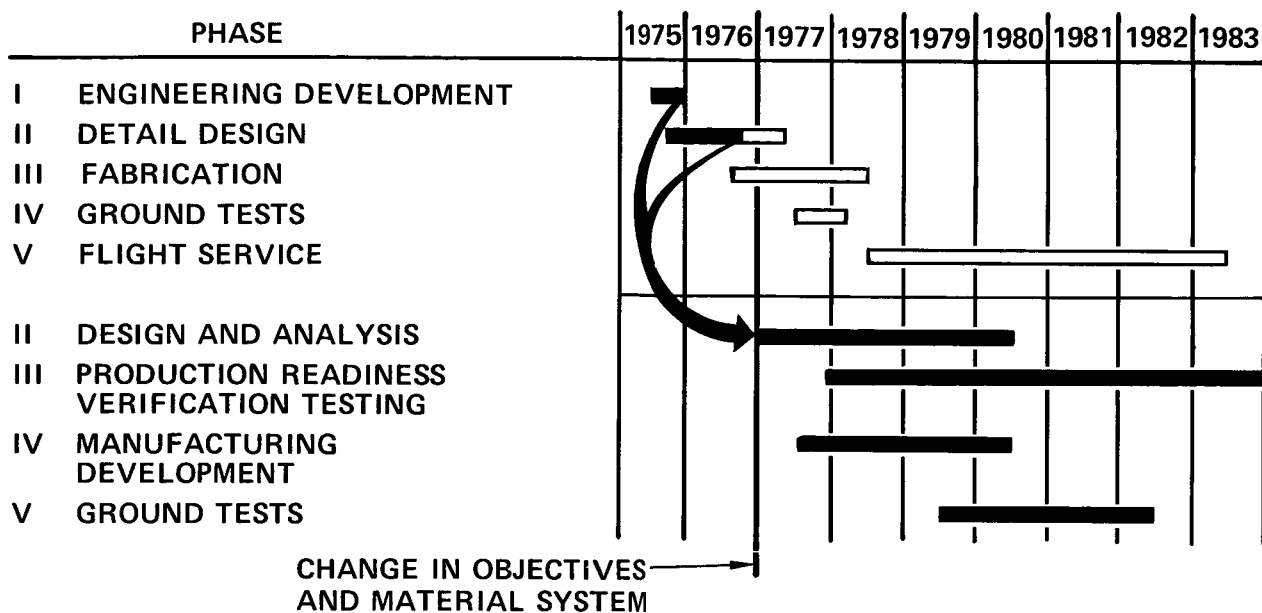


Figure 1. - Master schedule for restructured program.

Thermal analysis showed however that the T300/5209 material would be marginal in satisfying compressive requirements in some high temperature/conditions that might be encountered in service. Although this potential strength problem could have been off-set by detail redesign, it was jointly decided by NASA and Lockheed that it would be in the best interest of achieving program goals to change the material system. Several 350 °F cure resin systems were evaluated and NARMCO 5208, was selected in lieu of the NARMCO 5209 resin system.

The initial program plan included flight service, with periodic inspections. It was anticipated that airlines would commit aircraft which are used in routine operations to the program, for the purpose of obtaining that flight service evaluation. Although a considerable effort was expended in persuading airline companies to participate in the development program, it was soon recognized that the idea of evaluating composite primary structure on passenger carrying aircraft was not practical at that time. A more achievable program goal was to generate technology that would provide the confidence needed to commit the use of advanced composite materials for primary structures of future aircraft. Therefore, the ACVF program was restructured in order to accomplish the new program goals and to accommodate the material change.

At the time of restructuring Phase I, Engineering Development, had been completed; and Phase II, Design and Analysis, was in progress. Restructuring Phase II consisted of completing the detail design and analysis, characterization of the T300/5208 material system, initiating producibility studies, and

conducting material, process, and concept verification tests. The significant change to Phase II due to restructuring was the addition of the Producibility Studies Task to identify, develop, and verify low-cost manufacturing techniques, processes, quality criteria, and design refinements.

A phase added to the program in the restructuring was Phase III, Production Readiness Verification Tests (PRVT). These tests were designed to provide information to answer the following questions:

- What is the range of production qualities that can be expected for components manufactured under conditions similar to those expected in production, and how realistic and effective are proposed quality levels and quality control procedures?
- What variability in static strength can be expected for production quality components, and are the margins sufficient to account for this variability?
- Will production quality components survive extended time laboratory fatigue tests involving both load and environment simulation of sufficient duration and severity to provide confidence in in-service durability?

To provide data, 22 components of each of two key structural elements of the ACVF were fabricated for test. One element represented the front spar/fuselage attachment area, and the other element represented the cover/fuselage joint area. Ten of each element were static strength tested. Six of each element were durability tested for the equivalent of ten years of service and statically tested at NASA Langley Research Center to determine their residual strengths. The remaining six of each were durability tested for the equivalent of 20 years of service. Two of each of these last six were durability tested at strain levels 1.5 times those in the basic program. At the completion of 20 years the remaining specimens were statically tested at NASA Langley Research Center to determine their residual strengths.

Phase IV was the full-scale tooling and fin fabrication phase and Phase V involved the full-scale ground testing.

Throughout this program, technical information gathered during performance of the contract was disseminated throughout the aircraft industry and to the Government through quarterly reports and final reports for each phase of the program. All test data and fabrication data were recorded on Air Force Data Sheets for incorporation in the Air Force Design Guide and Fabrication Guide for Advanced Composites.

Use of commercial products or names of manufacturers in this report does not constitute official endorsement of such products or manufacturers, either expressed or implied, by the National Aeronautics and Space Administration. This report summarizes the major technical achievements of the program.

ADVANCED COMPOSITE VERTICAL FIN DESIGN

General Description

The fin box consists of 2 covers, 2 main spars, 1 stub spar and 11 ribs. An exploded view of the final design fin box is shown in figure 2. The box is 25 feet tall with a root chord of 9 feet and represents an area of 150 square feet.

Design Criteria

The fin was designed to meet several structural criteria. The primary criterion was that the fin be designed to carry the design loads during and after exposure to the environmental conditions encountered in worldwide service. The fin must demonstrate the ability to carry design ultimate load without failure and design limit load without permanent deformation. The fin must also demonstrate the ability to carry design limit loads after the failure of single critical elements of the structure. The fin must be capable of being installed on an L-1011 aircraft without compromising the other structure or affecting interchangeability. The fin must be functionally compatible with the surrounding structure.

The fin bending stiffness (EI) and torsional stiffness (GJ) must closely match those of the metal fin box so as not to change the aeroelastic response. No buckling may occur below design limit load. This limitation on buckling was imposed because there was very little data available on post buckling behavior.

Detail Design

The covers were designed primarily by stiffness. The skin tapers in steps from 34 plies at the root end to 16, 14, then 10 at the tip end. The edges were built up to 0.12 in. (24 plies) to allow for countersinking holes without feather edges. The skin contains only 0° and +45° plies in the layup as shown in figure 3.

The closed-hat section stiffener was selected because of its torsional stability and the fact that it did not have to be tied to each rib. The stiffener was built up of two 5-ply segments of (+45/0/+45) with a 10-ply segment of all 0° sandwiched between them in the crown. A short segment of 8-doubler plies was added only at the root end to stiffen the side walls for shearing out crown loads. Internal clips of two plies at +45 degrees were added to prevent peel.

The actuator ribs consist of a partial solid graphite web rib at VSS 90.19 and a combination solid graphite web and graphite cap aluminum truss rib at VSS 97.19. The solid web is a 16-ply layup (+45/0/-45/90₂/-45/0/+45)_s. The sides adjacent to the covers are flanged to provide part of the skin attachment. Additional cap is provided by a C-section consisting of a 19-ply

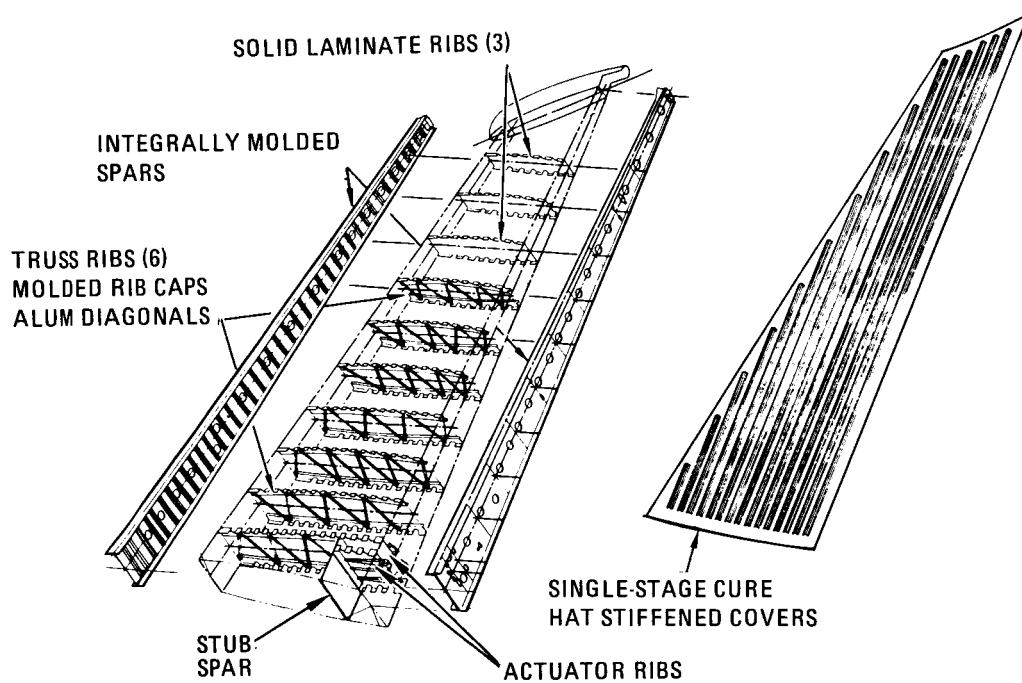


Figure 2. - Advanced composite vertical fin final design configuration.

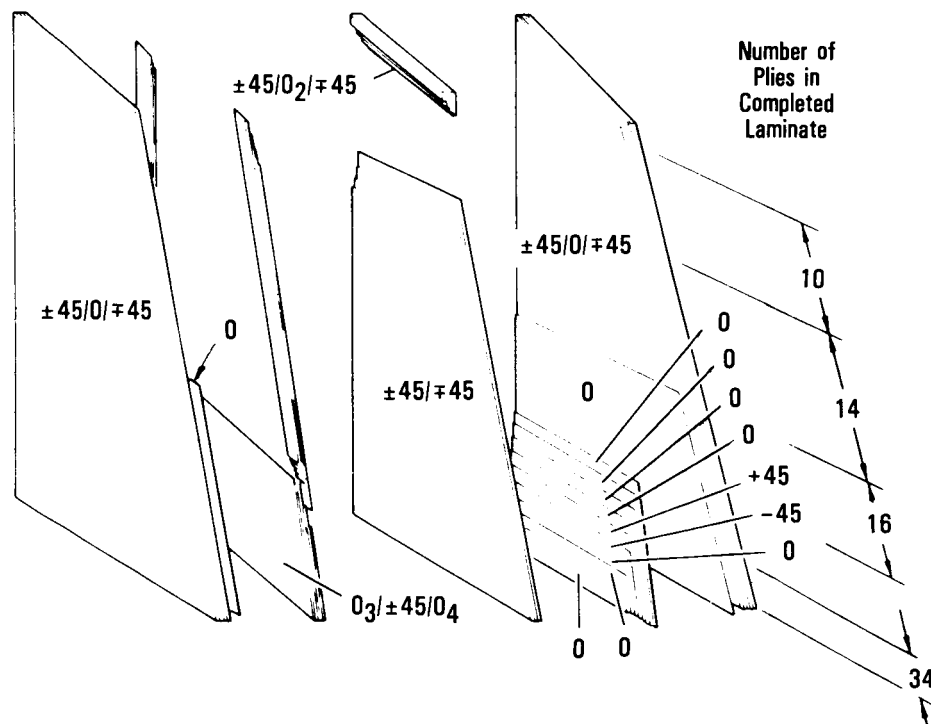


Figure 3. - ACVF skin ply buildup.

layup ($\pm 45/90/\mp 45/0/\pm 45/\bar{0}_3$). This cap extends the full length of the rib at VSS 97.19. The forward portion of this rib consists of graphite epoxy C-section caps and aluminum cruciform extruded truss members. The truss rib caps are C-section caps consisting of 19 plies with the same layup as the VSS 97.19 rib cap. The truss members are aluminum cruciform extrusions.

The solid web ribs are a sandwich design. The fin box becomes too shallow near the tip to use the truss design efficiently. The most cost-effective design is one without stiffeners. Because of the size of the rib web, an all graphite-epoxy shear buckling resistant design would be heavy. Thus, a syntactic epoxy core was used. Syntactic epoxy is an epoxy system filled with glass microballoons which has about half the density of graphite epoxy. The face sheets consist of seven plies laid up as $\pm 45/0/90/0/\mp 45$. The edges around the core are graphite epoxy laid up as $\pm 45/0_2/\mp 45$. The uncured syntactic core is 0.0375 in. thick and compresses down to about 0.03 in. during cure.

The front and rear spars similar in shape and size, were designed as one-piece components with cocured rib attach angles, stiffeners, caps, and webs. The front spar cap forward flange, rear spar cap aft flange, and the fuselage joint areas were configured to interface with the existing metallic structure and, therefore, do not necessarily represent the most efficient designs for advanced composite structures. Another critical interface area was the attachment of rudder hinges to the rear spar. To ensure that these locations were accurately maintained, separate aluminum attachment angles were jig located on assembly and mechanically attached to the spar.

Spar strength and stiffness were controlled by selecting ply layups with a sufficient number of ± 45 -degree plies in the webs to provide the required shear strength and 0-degree plies in the caps for axial loading. To facilitate fastener installation in the final assembly fixture, access holes were provided in the spar webs. Two access holes were required in each rib bay. The access hole edges were not reinforced.

The stub spar is located between the root closure rib and the rudder actuator ribs. It has been retained as an aluminum assembly.

Design Analysis

The internal loads and deflections for the composite fin were predicted using a three-dimensional NASTRAN model. Using this information a stress analysis was made of each component to determine the strains and the stability margins. Fail-safe analyses were performed with various structural members failed to verify that the remaining structure could sustain limit loads (considered as ultimate). A flutter analysis was also performed to verify that the flutter margins had been maintained or improved compared to the metal fin.

PRODUCIBILITY STUDY

A producibility and design-to-cost, cost reduction study was implemented after the program restructuring discussed in the introduction. Engineering manufacturing and tooling functions participated in the study.

Each fin component was analyzed to produce the lowest cost approach which would meet the structural requirements.

From this study, the cover configuration changed very little. The only significant item was the change from precured, secondarily bonded skin and stiffeners to the cocured design.

Channel type rib development - rib redesign.- A brief history of the truss rib cap design evolution is shown in figure 4 and described below in chronological order:

- Concept A: This is the original rib cap configuration. The design turned out to be highly complex and not cost effective.
- Concept B: In configuration, concept B is similar to concept A with the exception of a central bead which replaces the blade stiffener. The beads fabricated with this process experienced severe microcracking.
- Concept C: In this concept an attempt was made to break up the large amount of 0° fibers in the bead by interleaving half of the existing 0° fibers in the outer flange. Although these changes produced a more efficient beam, they also created a loss of bead definition and did not solve the microcracking problem.
- Concept D: This concept is similar to concept C except for the extra +45° plies added to the central bead to further break-up the concentration of 0° plies. This addition produced only slight improvement in over-all bead quality.
- Concept E: The shape of the rib cap in Concept E is a basic symmetric channel which is laid-up and cured on a single male tool. The loss in bending and axial stiffness is compensated for by distributing the 0° bead material of concept D evenly throughout the cross-section and by increasing the depth of the beam section. The small weight penalty experienced by this design was justified due to its greater producibility potential.

Solid web ribs.- The solid web ribs also underwent several design iterations aimed at making the ribs more producible. Figure 5 shows the design evolution of these ribs beginning with the earliest configuration.

- Concept A: This concept was the original solid laminate rib design. The longitudinal web stiffeners were configured as integral blades

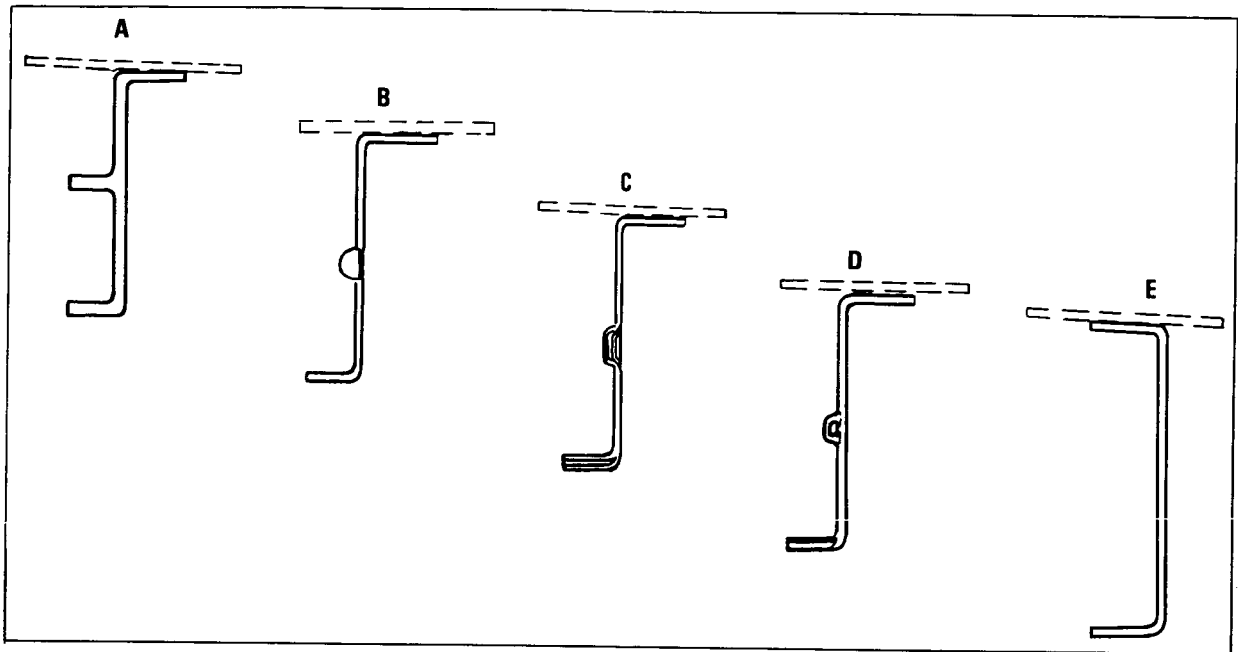


Figure 4. - Rib cap evolution.

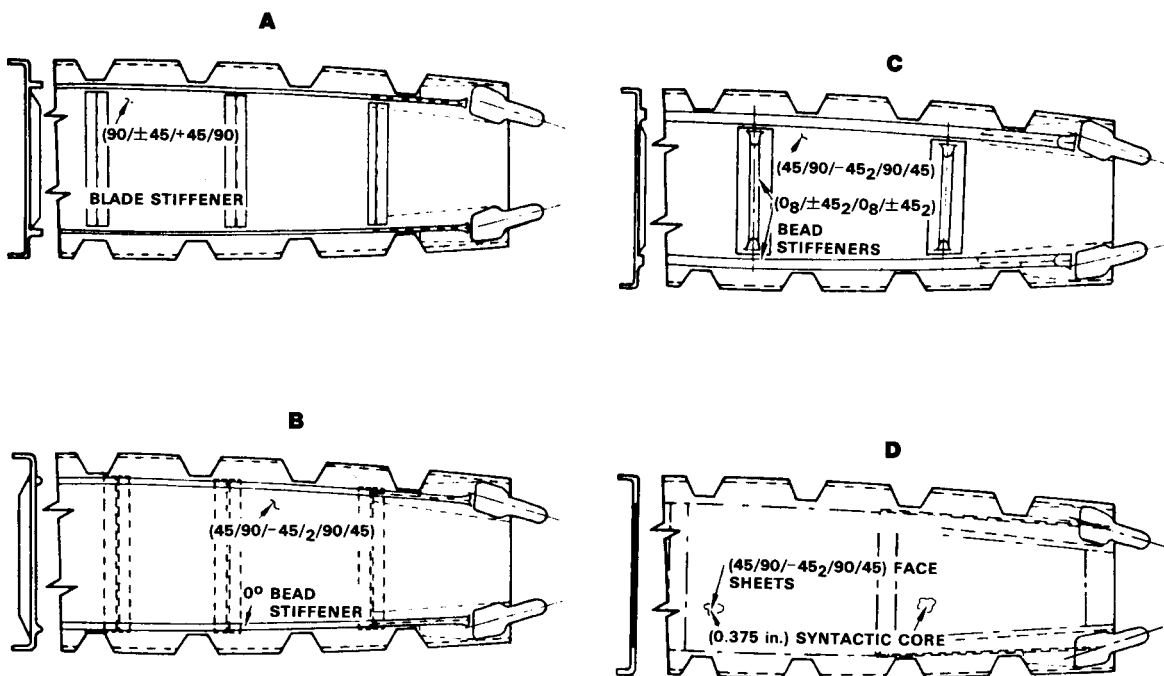


Figure 5. - Solid web rib evolution.

while the transverse Z stiffeners were secondarily bonded to the web. This design was not cost-effective.

- Concept B: This concept became the baseline and was considered a more producible design. The rib featured 0° longitudinal bead stiffeners combined with transverse T shaped stiffeners co-cured to the web.
- Concept C: This concept was introduced to correct for several producibility problems encountered in the manufacture of concept B. The principal problems concerned profile distortion, lateral shifting, and microcracking within the all 0° bead. To correct for these discrepancies, +45° plies were interleaved between the 0° plies in the bead. In addition, the "T" stiffeners were replaced with bead stiffeners and relocated on the same side of the web as the longitudinal bead for producibility reasons. Despite some minor improvements obtained as a result of these changes, none of the process verification rib specimens satisfied design standards.
- Concept D: This configuration featured a 0.0375 in. syntactic core and precluded the need for beads or external stiffeners. It manifested the best structural and producibility characteristics of the four concepts.

Numerous proposed spar design changes were evaluated for potential cost savings during the producibility studies. From these studies, three design changes were made in the Phase I spar design.

- Kevlar cloth was originally planned for the spar webs because of its lower material cost and the assumption that a thicker material (i.e., fewer plies) would be less expensive to lay up (figure 6). However, when the use of automated tape laying equipment was considered, together with revised projected material costs, unidirectional graphite/epoxy tape offered a substantial cost improvement.
- Detailed analysis of the web access holes revealed high strain levels at the edge of the hole at 45° to the spar center line. On the original design using Kevlar, there was an insufficient number of +45° plies in the web to withstand the strain, and unidirectional reinforcing rings were introduced (figure 7). When the change from Kevlar was made, however, additional +45° graphite/epoxy plies were added and the reinforcing rings were no longer required.
- Figure 8 shows the revised stiffener configuration resulting from the producibility studies. Analysis of this item indicated that a direct tie-in from stiffener to spar cap was not required to stabilize the web, and therefore the simpler stiffener configuration was incorporated.

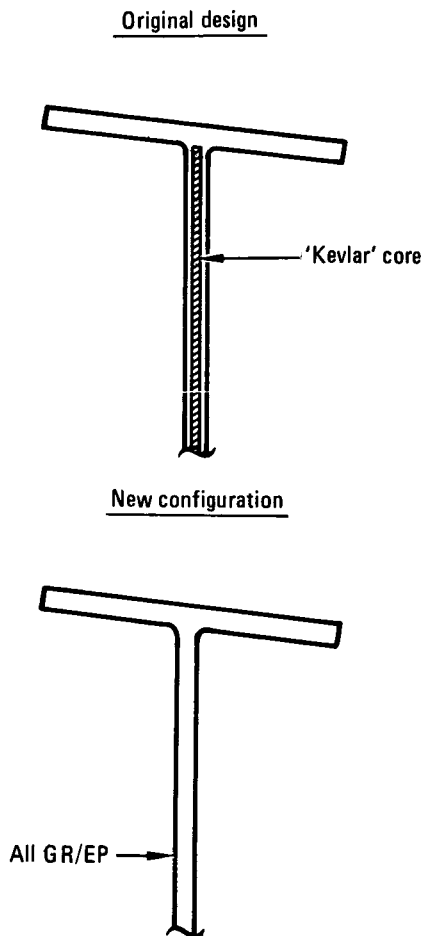


Figure 6. - Design changes, spar web material change.



Figure 7. - Spar web access hole.

PROCESS VERIFICATION

With design completed the development of the manufacturing process became the pacing task. The main task for cover fabrication was the development of the mandrels to support the prebled hats on the inside skin surface for cure. Solid rubber mandrels, foam rubber mandrels, and inflatable mandrels were investigated. The inflatable mandrels were selected because they offered more manufacturing flexibility. Cure cycle and bleeder/breather systems development completed the cover process development. The rib manufacturing process

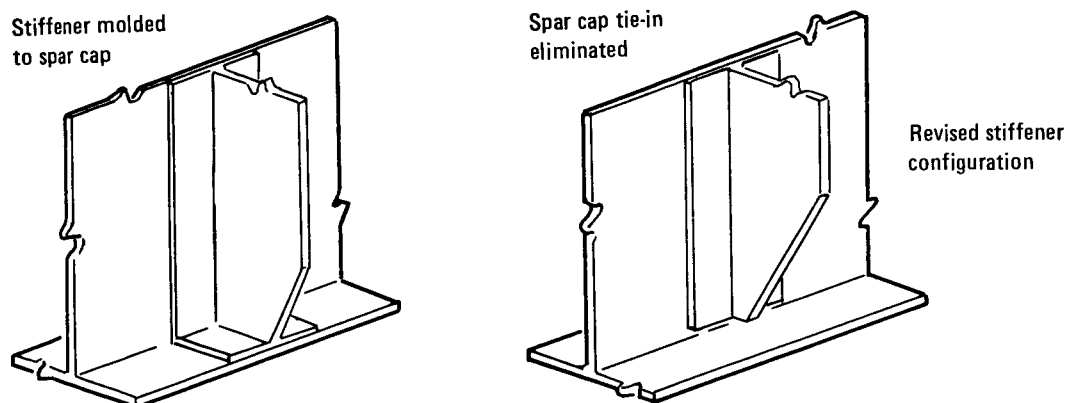


Figure 8. - Spar web stiffener.

development involved only developing the cure cycle and bleeder/breather systems. The spar process development involved primarily cure cycle and bleeding development. A small tool was fabricated to facilitate this development and to assess the details of the rubber which was used to provide pressure on the spar caps during cure.

ANCILLARY TEST PROGRAM

Material Verification

Basic design allowables were determined by a large number of coupon tests at several environmental conditions. Ply level data were obtained for use in the analytical determination of laminate data. The laminate data were then verified by tests of typical laminates. Factors were determined for environmental conditions, notches, and damage tolerance. Similar tests were performed on specimens representing various mechanical joints, to verify joint strengths.

The design temperature extremes for the fin are -65°F to 180°F and the various fluids include hydraulic fluid, paint stripper, and water. For the notched laminate condition a 3/16 in. diameter hole was used as this is representative of the most common fastener size in the fin box assembly. Impact and defect tolerance testing was also conducted.

The design allowables approach is illustrated in figure 9. The resulting allowables were presented as carpet plots. A sample carpet plot is shown in figure 10.

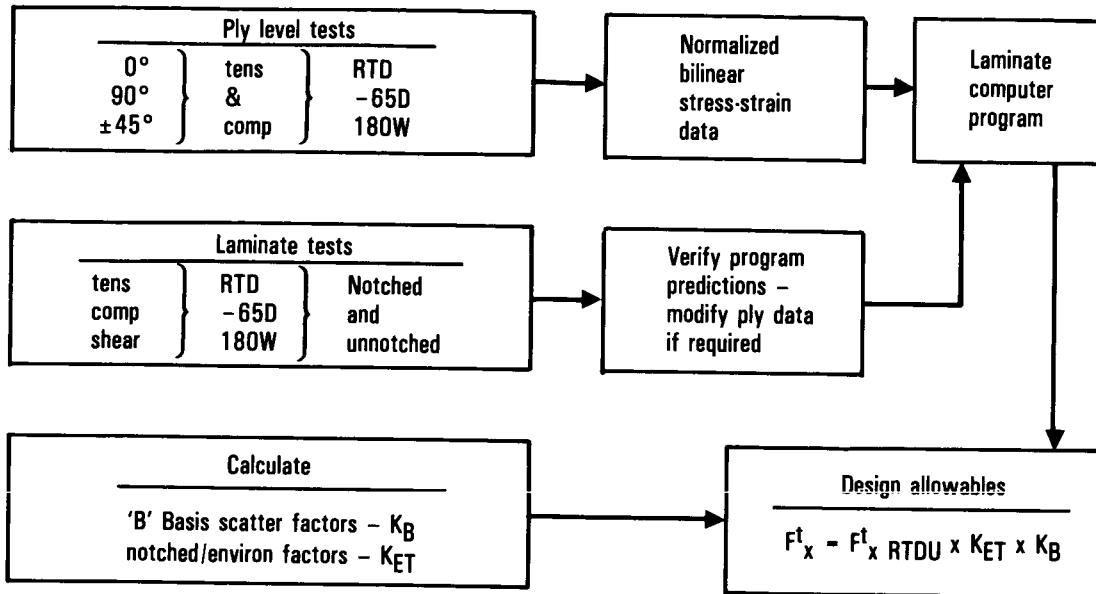


Figure 9. - Design allowables approach.

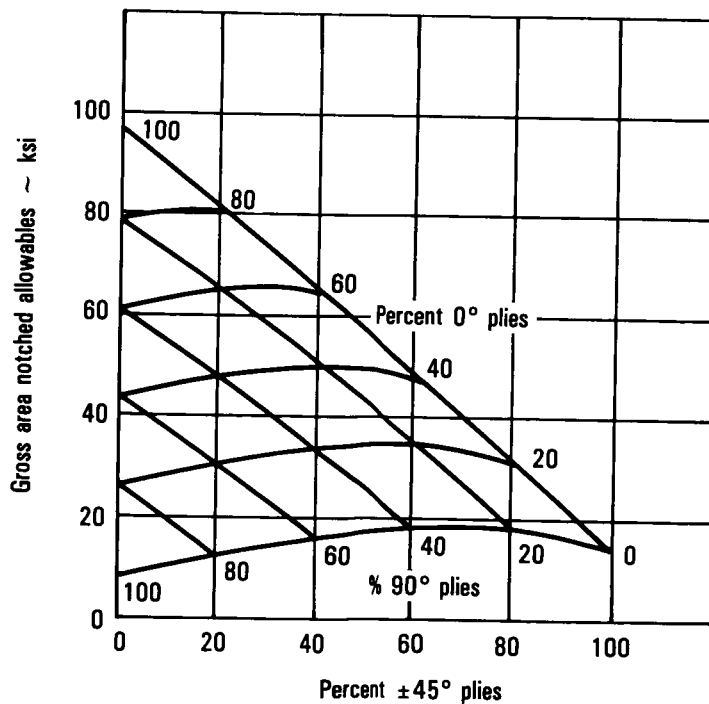


Figure 10. - T300/5208 unidirectional tape tensile strength design allowables.

Concept Verification

The objectives of the concept verification tests were to verify the structural integrity of the most critical areas of the fin and to verify the analytical methods. In order to meet these objectives, a series of tests were conducted on components of the cover, the spars, and the ribs. Static and spectrum fatigue specimens were tested under various temperature and moisture conditions. These tests were used to demonstrate a consistent performance in subcomponents designed using allowables derived from coupon and element data.

Subcomponents were moisture conditioned to a minimum of 1 percent weight gain in 95 percent ± 5 percent relative humidity at 150 F ± 5 F. The moisture weight gain was determined by weight-control coupons which accompanied the subcomponents.

Failure loads and modes were predicted by analyses and were compared with the test results. The test results are summarized in table I.

PRODUCTION READINESS VERIFICATION TESTING

The Production Readiness Verification Tests (PRVT) were performed on 22 components of each of two key structural elements of the ACVF. One element represented the front spar/fuselage attachment area, and the other element represented the cover/fuselage joint area. Ten of each element were static strength tested to determine the variability in static strength. The remaining twelve of each element were durability tested, six each for the equivalent of ten years of service and six each for the equivalent of twenty years of service. Residual strength testing was performed at NASA Langley Research Center.

Fabrication

The cover PRVT components were fabricated in the Lockheed-California Company (Calac) plastics production shop by production personnel with manufacturing research assistance. The PRVT spar components were fabricated in the Lockheed-Georgia Company (Gelac) manufacturing research shop using both production personnel and manufacturing research personnel. A typical cover component is shown in figure 11 and a typical spar component is shown in figure 12.

Twenty-eight cover components and twenty-two spar components were produced. Inspections showed that twenty-two of the cover components were acceptable for test and that all the spar components were acceptable. The scrap of 6 covers was mainly due to tooling problems which resulted in lack of pressure in some critical areas and caused porosity. One cover was scrapped because of a machining error and one because of foreign matter which was suspected to be backing paper.

TABLE I. CONCEPT VERIFICATION TEST RESULTS

Spec. Type	Size	Load Type	Condition	DUL	Failure Mode		% DUL	Observed Failure Mode	Comments
					Calculated	Actual			
Truss Rib Test	51 in. x 22 in.	Static Bending	R.T.D.	Combined Loads	170 lb/in	167 lb/in	—	Flange Bending	
Rear Spar Test	24 in. x 72 in.	Static Bending	R.T.D.	980 lb/in	1390 lb/in	1590 lb/in	163%	Shear at edge of lightning hole	
Rear Spar Test	24 in. x 72 in.	Static Bending	180°F Wet	980 lb/in	1340 lb/in	1770 lb/in	181%	Shear at edge of lightning hole	
Spar Web Test	24 in. x 24 in.	Static Shear	R.T.D.	52,000 lb	55,000 lb	59,000 lb	113%	Shear at edge of lightning hole	
Spar Web Test	24 in. x 24 in.	Static Shear	R.T. Wet	52,000 lb	55,000 lb	64,000 lb	123%	Shear at edge of lightning hole	5 thermal cycles 65°F to 180°F prior to test
Spar Web Test	24 in. x 24 in.	Fatigue Damage Tolerance	R.T.D.	52,000 lb	N.A.	60,400 lb	N.A.	Shear at edge of lightning hole	No damage growth in one lifetime
Front Spar Test	24 in. x 72 in.	Static Bending	R.T.D.	1305 lb/in	1565 lb/in	1680 lb/in	129%	Shear at edge of lightning hole	
Truss Rib Attachment Test	25 in. x 22 in.	Static Hinge Loads	R.T.D.	7100 lb	15,060 lb	19,500 lb	275%	Fasteners failed in double shear	No composite failure
Solid Web Rib Attachment Test	27 in. x 22 in.	Static Hinge Loads	R.T.D.	5170 lb	14,000 lb	—	—	—	No failure at 15,500 lb. Test suspended
		Fail Safe	R.T.D.	5170 lb	9720 lb	10,600 lb	205%	Tension in hinge lug	No composite failure

TABLE I. - (Continued)

Spec. Type	Size	Load Type	Condition	DUL	Failure Mode		% DUL	Observed Failure Mode	Comments
					Calculated	Actual			
Rib Attachment Test	31 in. x 11 in.	Static Actuator Loads	R.T.D.	15,920 lb	40,000 lb	—	—	—	No failure at 24,900 lb — capacity of loading system
		Fail Safe	R.T.D.	15,920 lb	30,000 lb	—	—	—	Element severed then loaded to 33,100 lb with no failure
Rib Attachment Test	31 in. x 22 in.	Static Actuator Loads	R.T.D.	±15,920 lb	37,000 lb	—	—	—	No failure at 38,600 lb — capacity of loading system
Surface Attachment to Fuselage Test	22 in. x 50 in.	Static Compression	R.T.D.	58,100 lb	78,000 lb	81,900 lb	141%	Buckles delaminated stiffener	Initial buckling occurred at 77% of DUL
Surface Attachment to Fuselage Test	22 in. x 14 in.	Static Tension	R.T.D.	77,400 lb	135,000 lb	221,500 lb	286%	Net tension	Retest of H25 but in tension
Stiffener Runout Test	7 in. x 50 in.	Static Tension	+180°F Wet	15,120 lb	24,900 lb	24,700 lb	159%	Fracture starting at fastener hole	Partial failure occurred at 21,000 lb
Stiffener Runout Test	7 in. x 50 in.	Fatigue	R.T.D.	15,170 lb	24,900 lb	—	—	—	Survived 2 life-times with no damage
Surface Panel Stability Test	21 in. x 75 in.	Residual Static	-65°F	15,120 lb	—	21,600 lb	142%	Hat/skin separation	
		Static Compression	+180°F Wet	58,100 lb	80,000 lb	70,000 lb	120%	Buckles delaminated stiffener	Initial buckling occurred at 93% of DUL

TABLE I. - (Concluded)

Spec. Type	Size	Load Type	Condition	DUL	Failure Mode		% DUL	Observed Failure Mode	Comments
					Calculated	Actual			
Surface Panel Stability Test	21 in. x 55 in.	Static Compression	R.T.D.	58,100 lb	80,000 lb	81,200 lb	140%	Buckles delaminated stiffener	Retest of H27
Surface Panel Fail-Safe Test	36 in. x 75 in.	Fatigue Damage Tolerance	R.T.D.	N.A.	N.A.	N.A.	N.A.	N.A.	Survived 1-1/2 lifetimes
Lightning Strike Test	48 in. x 22 in.	Lightning Strike	R.T. Wet	N.A.	N.A.	N.A.	N.A.	Local resin burned away (1-1/2 in. dia) partially through thickness. Minor delam. surface ply	C-Scan showed no additional damage. Coupons will be cut for static tests

DUL Design Ultimate Load
 RTD Room Temperature Dry
 RT Wet Room Temperature Wet
 NA Not Applicable

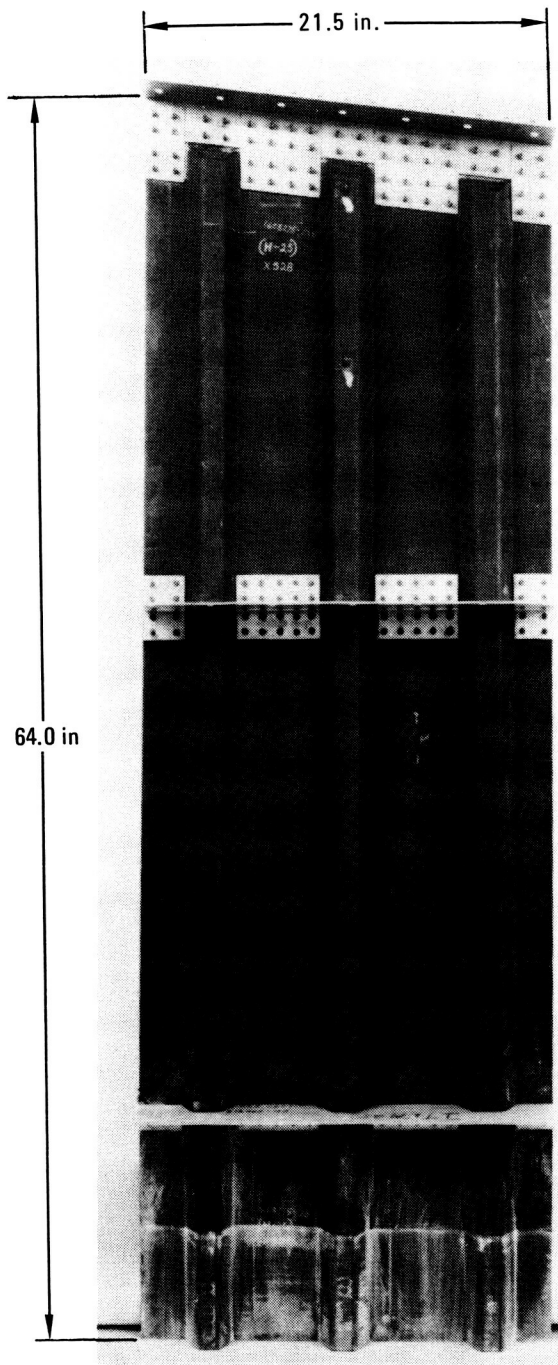


Figure 11. - Typical cover specimen.

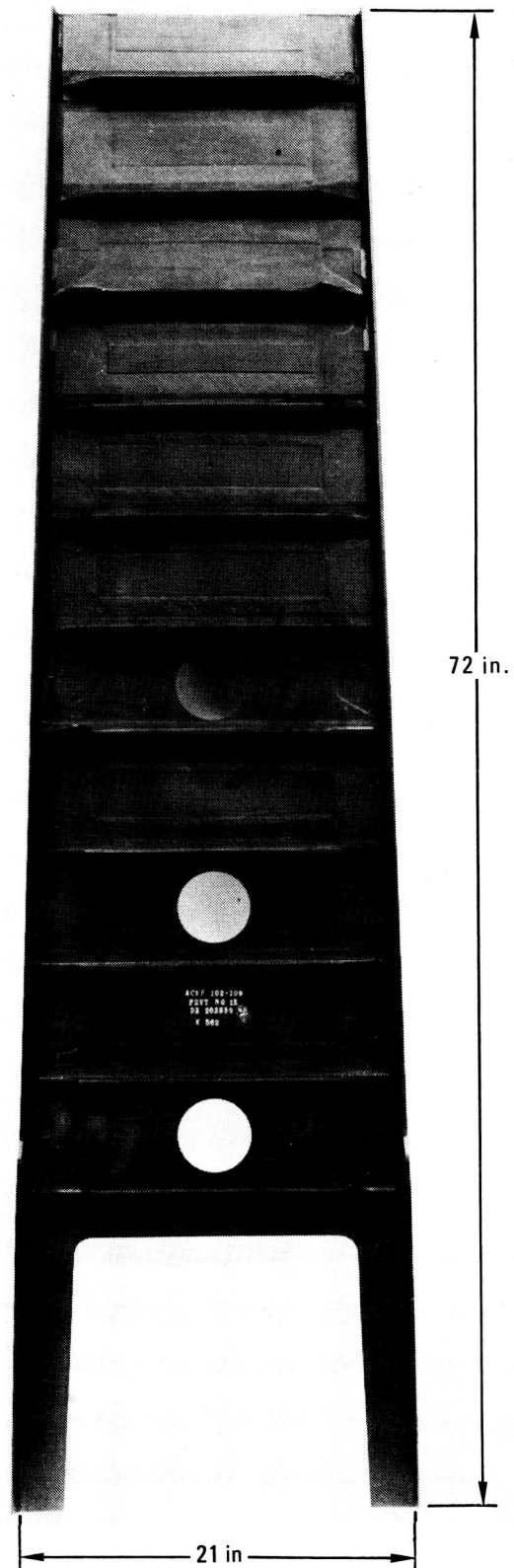


Figure 12. - Typical spar specimen

A review of the inspection results shows that the ultrasonic inspection techniques successfully screened components containing porosity, voids and foreign matter. Resin contents and thickness correlated except in areas of porosity. Thickness check of a cured part proved to be a good early indicator of the quality of a part.

Thus the answer to question one concerning production quality is as follows:

The range of production qualities that can be expected for components manufactured under conditions similar to those expected in production has been established. The spars were produced using tooling which underwent only minor modifications during the run of 24 components, similar to a production run. The covers were fabricated using tooling that underwent various modifications during a run of 28 components. Thus extremes of the production environment were encountered.

The quality control procedures used proved adequate in identifying discrepancies. In particular NDI techniques developed and refined during the program worked very well. The mechanical process control tests proved to be of varied effectiveness individually but when viewed on a combined basis for each component correlated well with NDI and physical tests.

Static Tests

Static tests were performed on 10 cover components and 10 spar components in the as manufactured condition. Figure 13 summarizes the results of the ten cover tests and shows the coefficient of variation. The 3.28 percent coefficient of variation for ten cover specimens represents very consistent test results for compression-loaded specimens (see table II). The predicted failure load was 78,100 lb., and the design ultimate load is 54,600 lbs.

Figure 14 summarizes the results of the ten spar tests and shows the coefficient of variation. The 6.11 percent coefficient of variation obtained for the ten spars is similar to test results achieved on numerous other composite and metallic test specimens (see table II). The predicted upper jack load at failure was 24,900 lb. The reference upper jack load corresponding to design ultimate load is 20,715 lb.

Thus the answer to question two concerning variability of static strength is as follows:

The static test results showed excellent uniformity. The coefficients of variation (CV) compare favorably with those of other common structural materials as shown in table II. The allowables used were derived from coupon data and the CVs of some of these data are shown in table II also. The failure modes of the covers and spars are influenced primarily by stiffness. The specimens in all cases failed at loads higher than predicted. The allowables used for prediction were based on average coupon data whereas design

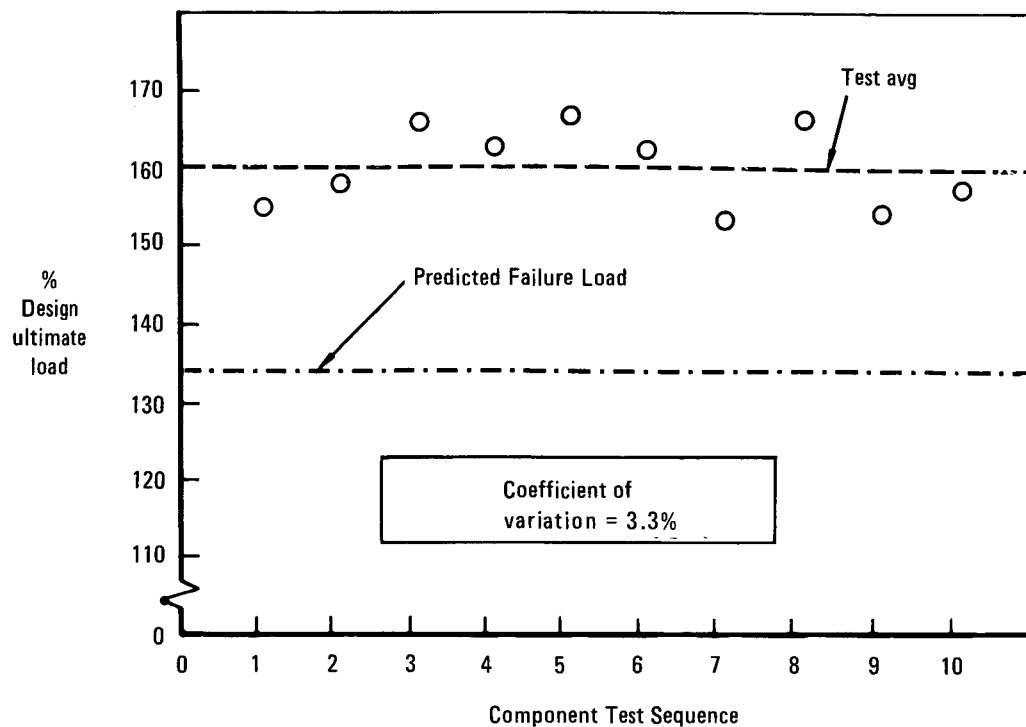


Figure 13. - Cover static test results.

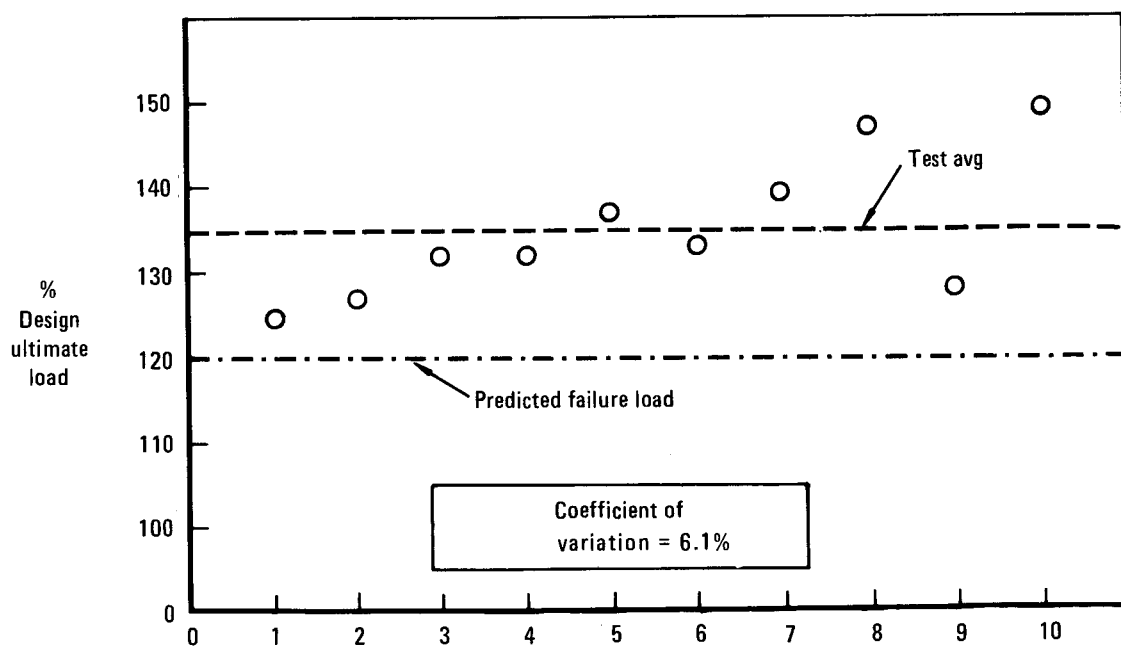


Figure 14. - Spar static test results.

TABLE II. - COEFFICIENT OF VARIATION IN STATIC STRENGTH OF SOME STRUCTURAL MATERIALS (REFERENCE 6)

Material	Component	No. Spec.	Loading	Coefficient of Variation (Percent)
Graphite-Epoxy	PRVT-Cover	10	Compression	3.3
Graphite-Epoxy	PRVT-Spar	10	Bending	6.1
Graphite-Epoxy	Spoiler	15	Bending	6.6
Graphite-Epoxy	Laminate Coupons	411	Tension	5.7
Graphite-Epoxy	Laminate Coupons	411	Ten-Modulus	4.0
Graphite-Epoxy	Laminate Coupons	290	Compression	9.0
Graphite-Epoxy	Laminate Coupons	290	Compr-Modulus	5.2
Wood	Mosquito Wings	5	Bending	10.3
Wood	Plywood Shear Wall	27	Shear	9.7
Concrete	Test Cylinders	216	Compression	10.6
Aluminum	7049-T73 Die Forging	384	Tension	3.2
Aluminum	A357-T6 Casting	804	Tension	5.5
Titanium	TI-5AL-2.5SN Sheet	565	Tension	3.9
Steel	Structural Steel	3982	Tension	7.1
Steel	17-7PH Sheet	88	Tension	5.1

allowables are statistically reduced below those levels. The allowable thus proved adequate to account for structure static variability.

Durability Tests

The durability testing was designed to give quasi-real-time results and to effectively bridge the gap between accelerated testing of coupons, which are completed in a matter of a few weeks and the real-time exposure of structural components in flight service.

The normal ground/air/ground environment causes both absorption and desorption of moisture by the epoxy matrix. This causes a laminate to swell and shrink in thickness. Such an effect would be most detrimental in joint areas where it might loosen the joint over a period of time.

An environmental spectrum was developed based on flights between Las Vegas and Miami in the summer. Both cities are hot, but Miami has a very high humidity, while Las Vegas has a very low humidity much of the time. The environmental cycle is shown in figure 15. One lifetime is represented by 5800 environmental cycles. Some cycles to higher temperatures, 160 F and 180°F are distributed through the test to represent the maximum expected

infrequently in service. Fatigue loading cycles are applied as shown in figure 15.

The durability specimens were set-up in chambers with six components in each chamber mounted in pairs. The set-up of six covers in one chamber is shown in figure 16 and the set-up of six spars in one chamber is shown in figure 17. Ten covers and ten spars were subjected to spectrum fatigue loading representing the ACVF. Two covers and two spars were tested at strain levels 1.5 times that of the basic components.

Six covers and six spars were taken out of the chambers after the equivalent of 10 years of flight service. These components were shipped to NASA Langley Research Center for residual strength testing. The two high strain spars failed just prior to the 10 year mark during the application of the highest load cycle. These spar had seen several applications of high loading during deflection surveys run some weeks prior to failure. The failure occurred at approximately 112% of the basic design ultimate loading. The spars had previously withstood nine applications of load between 116 and 120% DUL. The conclusion was that delamination started and grew to catastrophic proportions due to several applications of load above the buckling threshold. The spar was not designed for post buckled loading.

The remaining four spars and six covers, including the two higher strain covers, were cycled to the equivalent of 20 years of service. These components were then removed from the chambers and shipped to NASA Langley Research Center for residual strength testing.

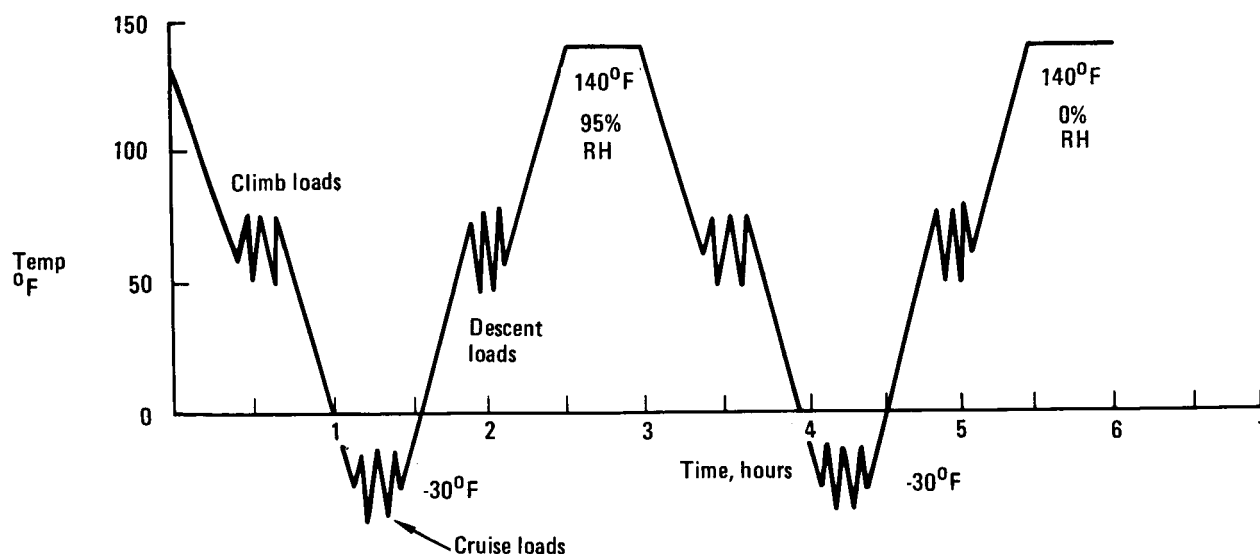


Figure 15. - Schematic of loads/thermal cycle for PRVT.



Figure 16. - Six covers in an environmental chamber.



Figure 17. - Six spars in an environmental chamber.

Thus the answer to question three concerning long term durability is as follows:

No evidence of degradation occurred during the durability testing. The results of the residual strength tests on the covers and spars are summarized in figures 18 and 19 respectively. Also shown in these figures are the static test results from figures 13 and 14 for comparison purposes. It is evident from this comparison that there was no loss in strength in the composite structure after the equivalent of 20 years of simulated airline service.

FIN FABRICATION

Tooling and processing parameters were developed for the composite fin. These procedures were used to fabricate the PRVT covers and spars and the components for two complete full-scale fin boxes.

Tooling

The cost of cover cure tooling was held to a minimum by designing a female cover assembly bonding fixture, which made it possible to use a one-piece contoured tool surface that did not require machining. A male tool would require various level caul surfaces to support the hat stiffeners, fillers and doublers in addition to the skin layup. Additional advantages of female tooling were contoured external skin surface smoothness and a less complex hat stiffener internal support system during cure.

Inflatable molded rubber mandrels (open to autoclave atmosphere) were developed to provide internal support and pressure application for the cover assembly hat stiffeners against the tooling hat caul plates. Cover assembly hat stiffener caul plates were constructed by hydraulically formed sheet steel.

Elastomeric tooling for the spars is a closed mold concept with internal, heat-expandable silicone rubber mandrels. The tool is illustrated in figure 20. Its base is essentially flat with all components of the tool and the composite spar assembled on this base in the proper sequence. Following assembly of these details, the tool cover, containing a cavity properly sized to contain the internal tool and part components, was lowered onto the base. The cover and base were accurately indexed by a novel key and slot arrangement, integral with the base and cover, respectively. A vacuum and autoclave pressure, in combination with heat-expandable rubber, applied the proper pressure to the spar during cure.

The major elements of the tool, shown in figure 20, consist of the cover, base plate, cap rails, rubber mandrels, and island blocks. Appropriately spaced bleed-holes in the cap rails and island blocks provide paths between the laminate and the bleed cavities where excess resin was collected.

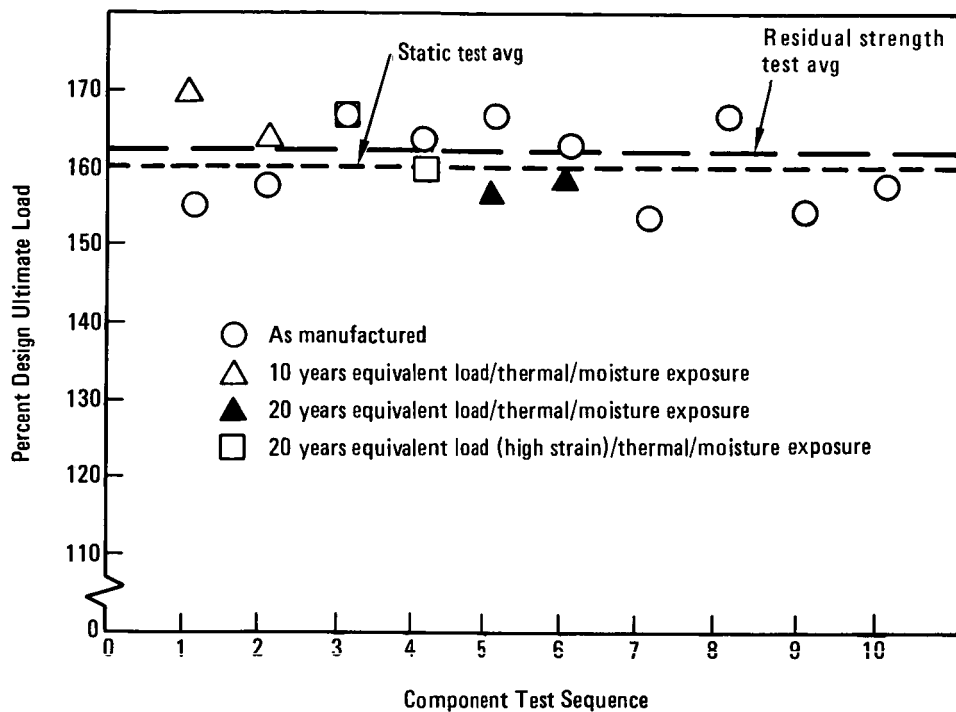


Figure 18. - Residual strength tests on PRVT covers.

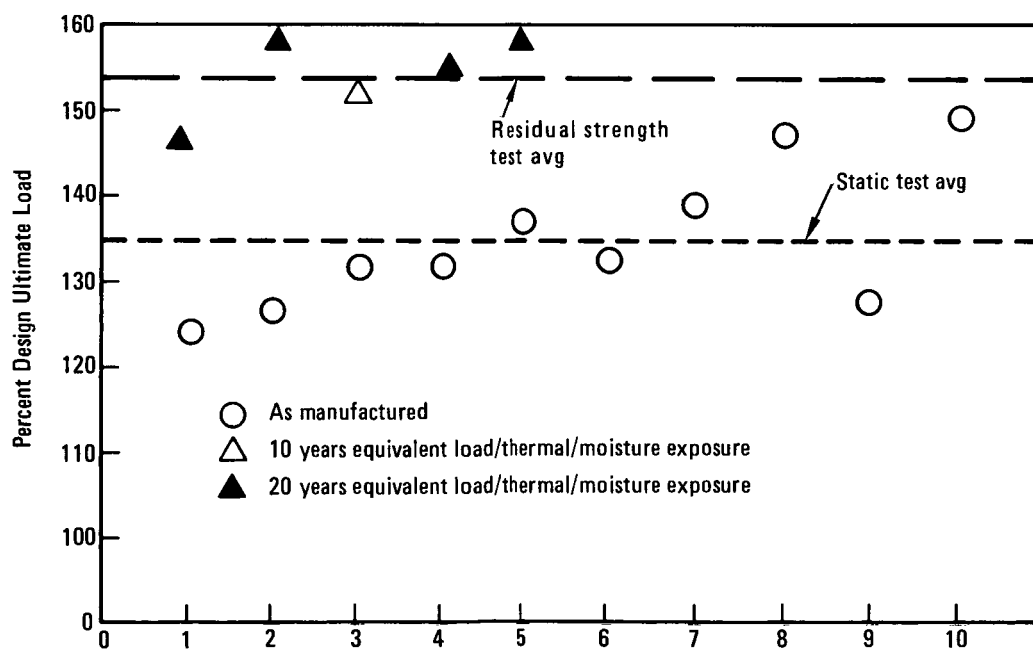


Figure 19. - Residual strength tests on PRVT spars.

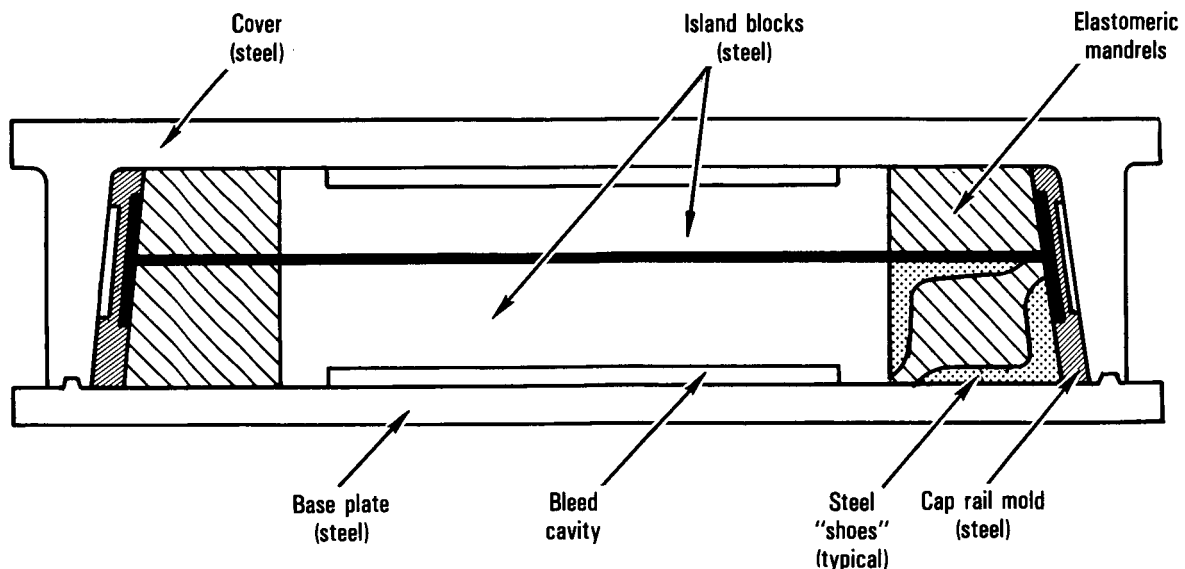


Figure 20. - Diagram of composite spar molding fixture.

The rib cap layup tools were conventionally machined from solid alphase cast aluminum tooling plate with pockets on the bottom side of the tool to reduce the heat-up time and provide even heat-up. Thermocouples and a vacuum system were made an integral part of the tools. To reduce the cost of machining the tools, the flange angle variances from front to rear spar ends of the tools were averaged to a mean angle.

The truss and actuator rib assemblies were assembled on wooden frame bench type assembly fixtures. The aluminum angle locators for indexing and clamping the rib caps and webs were set to engineering master drawing photographs on metal template stock fastened to plywood backing.

The composite fin box was assembled at the production L-1011 empennage assembly plant in Meridian, Mississippi. One of the L-1011 metallic fin assembly fixtures and other related tools were reworked for use in the assembly of the composite fin. These tools were converted back to their original condition after the composite fins were assembled.

DETAIL FABRICATION

Covers

The cover assemblies consisted of the skin plies, doublers, fillers, and hat stiffeners that were laid up manually and cocured as follows:

Cover fillers: The cover fillers were laid up in sheet size and trimmed to net size per a layout template. The fillers consist of 10 and 18 plies, oriented at +45 and -45 degrees, alternately. The root end fillers were step tapered and contained eight additional plies.

Cover hat stiffeners and reinforcing straps: The cover hat stiffeners were laid up on layup blocks using four preplied groups. The hat stiffeners were then trimmed to net width using trim templates. The reinforcing straps were also preplied, trimmed by hand, and B-staged. The straps consisted of a +45-degree and a -45-degree ply.

Cover assemblies: The cover doublers were preplied and laid up on the metal bonding fixture (MBF) with the skin plies. The hat stiffeners and straps were fitted on the mandrels, placed in the hat cauls, and the loaded cauls located on the MBF. The assembly was then bagged and subsequently cured in the autoclave.

Conventional cure bleeder stacking is shown in figure 21. Data from tag-end test results showed the resin content to be below the minimum requirements at the root end. Therefore, the peel ply was removed from the root-end bleeder stacking in this specific area of the hat cover, raising the resin content. Curing of the covers was accomplished in an autoclave at 350 F.

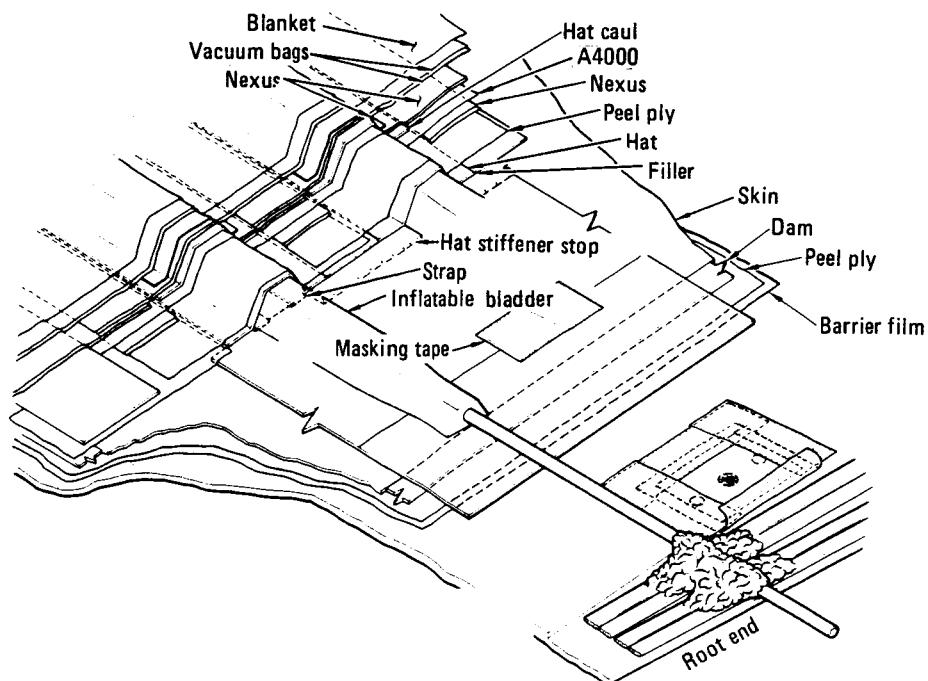


Figure 21. - Typical hat/skin assembly cure stacking arrangement.

Spars

The numerous plies used to build up the spars were laminated, trimmed, and assembled into caps, rib angles, stiffeners and webs, and loaded into the spar tools for initial cure in the autoclave. Process control specimens were taken from the spar webs and tag ends to verify physical and mechanical properties.

Procedures for laying up broadgoods and cutting out the various patterns were similar for both the front and rear spars. These layups are easily adaptable to automation and computer-derived ply patterns. The front spar had six plies of $+45$ -degree ply orientation on the outer faces of the web. Both faces can be laid up as a 6-ply-wide laminated sheet, and a pattern can be used to cut the two outer faces of the spar web. Similar groups of ply orientations were used for the remaining elements of the spar webs and for all of the other elements used to assemble the spars.

These spar elements were put together in kits and partially assembled. First, the preassembled stiffeners and rib attaching angles were placed in their locations, as shown in figure 22. Next the spar web was located on top of the stiffeners, using tooling pins.



Figure 22. - Loading stiffeners in front spar tool.

After the web was in place, a sheet of Armalon was placed on top of the web to provide a breather between the web and island blocks. The 6 plies of +45 degrees on the outer faces of the spar web extend along the lengthwise edges of the spar. These plies are folded and trimmed to form the inner flanges of the spar caps. The cap rail molds containing the remaining cap plies were then placed in position completing the assembly. The cover was placed on top of the assembled spar and the large number of thermocouples were carefully routed through the vacuum bag.

The spar was then cured at 250°F in the autoclave. After cure the tooling was disassembled and the spar placed in an oven for postcure at 350°F.

Ribs

The material for the ribs was cut and preplied in three- or four-ply stacks. These stacks were then positioned on warmed aluminum tools that had baked-on release coat. After positioning each preplied stack, the material was vacuum debulked. At the completion of layup, the flanges were trimmed back to be 0.5 in. above the tool base plates. The laminate was then lifted off the tool and a barrier film draped over the tool. The laminate was then replaced on the tool.

The bleeder stacking for the rib components was developed to accommodate a standard autoclave cure cycle for the four configurations of rib components. Figure 23 shows the solid web bleeder stacking arrangement. The bleeder stacking arrangement for the balance of components is depicted in figure 24. The solid web stacking differs from other rib stackings to accommodate bleeding from both sides of the core in the solid web rib. All composite rib components were cured in a space-heated autoclave pressurized with CO₂.

ASSEMBLY

Subassembly of Spars

The assembly of the rear spar required 21 metal stiffeners, angles, clips, and fittings to be installed with approximately 500 fasteners. A similar number of parts and fasteners were used in the subassembly of the front spar. Metallic parts were painted with an epoxy primer and white, polyurethane top coat. Faying surface sealants were applied before permanently installing fasteners.

Assembly of Fin Box

Assembly of the first L-1011 composite fin box proceeded smoothly and efficiently. The first step in assembly of the fin box was to load the front spar in the assembly fixture.

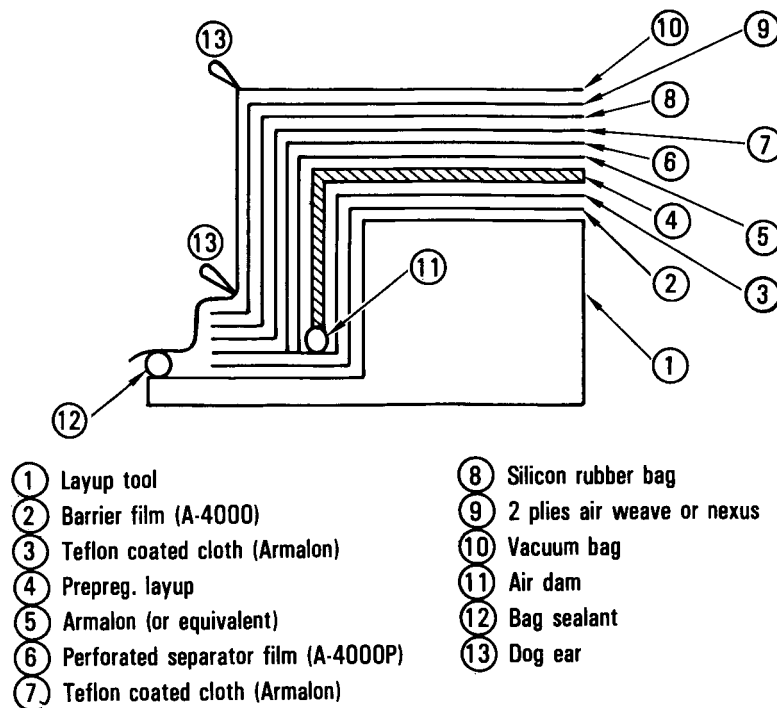


Figure 23. - Solid web bleeder stacking arrangement.

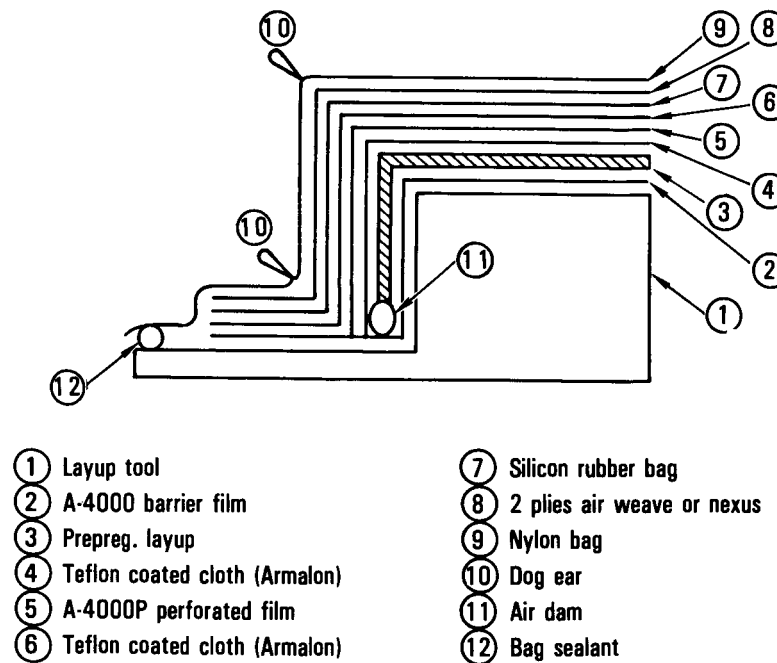


Figure 24. - Actuator and truss rib bleeder stacking arrangement.

Next, the ribs were loaded in the assembly tool and temporarily attached to the front spar. Some minor discrepancies were found during fit-up, and these were corrected by minor rework of the rib flanges and by relocation of pilot holes.

After the ribs were loaded, the rear spar was installed as shown in figure 25. The spars and ribs were permanently attached using titanium HL12 Hi-Loc pins and stainless steel HL94 collars. No significant problems were encountered during the assembly of the spars and ribs. The problems that occurred were typical pilot hole mislocations, gaps, and design errors, and these discrepancies were not attributable to the composite structure.

After the ribs and spars were attached permanently, the right-hand cover was loaded to the spar-rib framework, drilled and marked for trim. The temporarily installed right-hand cover was attached with clecoes. With the right-hand cover in place, the left-hand cover was loosely loaded and marked. The right-hand cover was removed and trimmed while the left-hand cover was being drilled. The right-hand cover was reinstalled, and the left-hand cover was removed for trim. The right-hand cover was permanently attached with HL13V Hi-Loc titanium pins and HL94 stainless steel collars.

Numerous small discrepancies typical of a first article fin assembly were uncovered, and practically all of these were in the metallic parts. No major problems were encountered. Discrepancies in the composite structure were easily disposed of with practically no loss of production time.

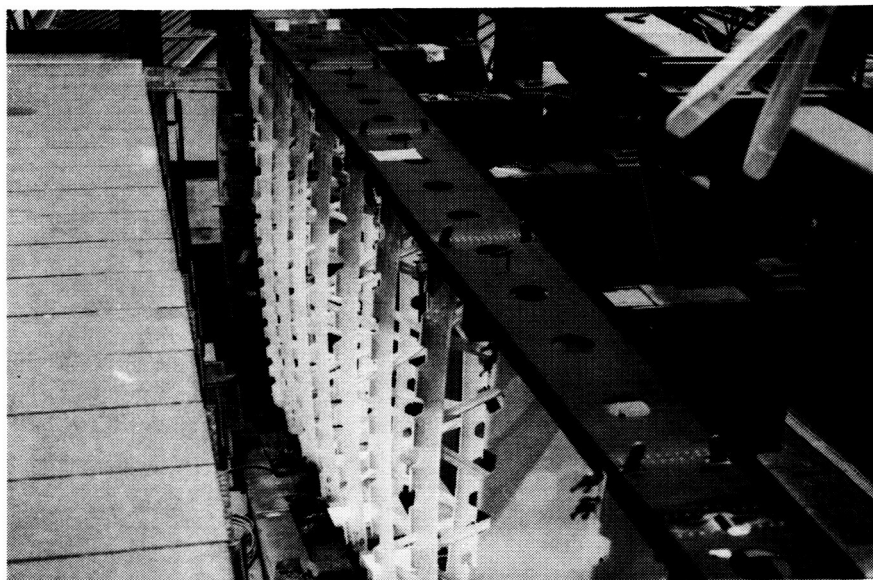


Figure 25. - Installation of rear spar.

The left-hand cover was permanently installed with titanium pins, stainless steel collars, and MS21140 blind fasteners in the upper three solid ribs. Final close-out of the fin box required working inside the box. The completed fin box was loaded on a specially designed, shock-mounted dolly shown in figure 26 for shipment to Lockheed-California Company's test facility for ground testing.

A second fin box was then assembled at Meridian. This box was identical to the first, both in assembly procedures and in instrumentation. Although start-ups, slow downs, and reschedules occurred during assembly of the second box, discrepancies and costs followed the typical drops expected on the learning curve of a second article.

QUALITY ASSURANCE

The traceability requirements for all parts and assemblies were achieved through (1) supplier material certification, (2) material acceptance test certification, (3) in-process documentation on shop orders, and (4) FAA conformity certification. In-process traceability was achieved by recording material batch number and roll number on the applicable shop order. In addition, processing information of particular concern to ensure product integrity, such as material out time, and autoclave functions of temperature, time,

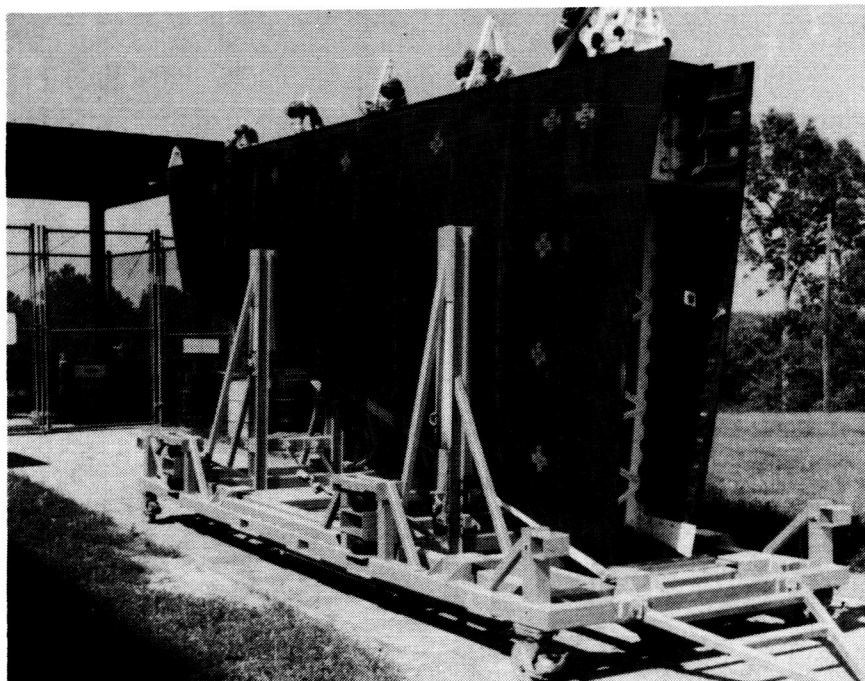


Figure 26. - Shipment of fin box on specially designed, shock-mounted dolly.

and pressure, were recorded on the shop orders. All inspection tags processed by the Material Review Board were recorded on the shop orders and filed by the Inspection organization. the shop orders show a complete record of the production and inspection activities performed to produce the hardware and are retained as a permanent record of all detail parts and assemblies.

The following rejection history covers the fabrication of rib components and covers to the point where apparent changes in the graphite prepreg material caused process/cure problems. A tabulation of the various causes for rejection is shown in table III. It should be noted that rejections caused by tooling and process development are included in the rejection statistics. No spars were rejected. Only minor tolerance discrepancies were found.

Workmanship rejections included such things as incorrect layup, incorrect trim, and mislocated holes. Corrective action in these instances was achieved by giving better instructions to manufacturing personnel and by providing foolproof tools. Process-related rejections included such things as broken vacuum bags, low resin content, low mechanical test results, and porosity and voids identified by nondestructive inspection (NDI). The problems of vacuum bag failures were virtually eliminated by removing sharp corners from the tooling and retraining manufacturing personnel. Adjustments were made during the process development phase to correct out-of-tolerance conditions noted by the test lab and NDI. Tooling errors were dimensional and affected either contour or trim. The tools were corrected, and subsequent parts were

TABLE III. - CAUSES FOR REJECTION OF RIBS AND COVERS

	VOIDS	FAILED LAB TEST	AUTOCLAVE FLAME OUT	VACUUM BAG BROKE	WORKMAN- SHIP	MISC.
TRUSS RIBS (2 CAPS)						
45 FABRICATED						
9 SCRAPPED		2	2	2	3	
SOLID WEB RIBS (1 PIECE)						
14 FABRICATED						
5 SCRAPPED	1	1	1		1	1
ACTUATOR RIBS (1 WEB, 2 CAPS)						
36 FABRICATED						
20 SCRAPPED	8	6		3	1	2
COVERS						
7 FABRICATED						
3 SCRAPPED	3					
TOTALS	12	9	3	5	5	3

dimensionally correct. The final two actuator rib components were not refabricated because of material problems.

One cover assembly was scrapped because of severe porosity and mark-off at the front and rear spar interface areas. The severe porosity problem was caused by a leak in the vacuum bag and a leak in an inflatable mandrel. The porosity areas were identified by ultrasonic inspection and confirmed by the QA laboratory after viewing core plugs with a 40x microscope. The problem was corrected by employing a double-bag procedure and performing high-pressure tests on the mandrels. The mark-off at front and rear spar interface area was caused by using several individual caul plates running along the front and rear spar interface areas. This condition was corrected by providing one-piece caul plates for both the front and rear spar areas.

Two other cover assemblies were both scrapped because of severe porosity. The porosity was due to an incoming material variation which was not detected during receiving inspection.

MANUFACTURING COST ANALYSIS

One of the major goals of the ACVF program was to demonstrate cost competitiveness with the metal fin. Therefore, a comprehensive producibility/design-to-cost (DTC) plan was prepared outlining the basic steps necessary to achieve that goal. The aggressive execution of that plan resulted in a successful program and achievement of the goal. An important part of that task was to obtain manufacturing cost data in sufficient detail to establish the production costs and compare the data with prior projections.

Cost tracking for the DTC program was performed by the Engineering Branches of both Lockheed-California and Lockheed-Georgia. Manufacturing had the prime responsibility for the cost projections. Lockheed-California had responsibility for the covers, ribs, common items, and the overall DTC program. Lockheed-Georgia had responsibility for the spars and final assembly. The Phase III Production Readiness Verification Test Program PRVT provided useful information on cost trends and learning curves because of the more than 20 cover and spar components fabricated. Data obtained from Phase IV fabrication also contributed to the determination and verification of costs.

The results of the Producibility/Design-to-Cost program are summarized in table IV. Projected costs based on time standards are shown for the baseline metal fin, which is the target, and for the ACVF, using both existing manufacturing methods and automated methods. Cost projections shown in the table were made by Manufacturing. ACVF costs based on actuals using existing manufacturing methods are also shown. They represent the cumulative average cost for 100 units in 1983 dollars. ACVF existing manufacturing methods include hand layup, stacking, trimming, and drilling. ACVF automated manufacturing methods involve numerical controlled tape layup, machine cutting, purchased preplied broadgoods, automated roll forming of hat stiffeners, platen press cured rib components, and powered gantry drilling for truss ribs.

TABLE IV. - COST COMPARISON - SUMMARY

	CUM AVG COST FIRST 100 UNITS 1983 \$	COST RATIO
• METAL FIN	\$198,300	1.0
• ACVF - EXISTING MANUFACTURING METHODS	178,400	0.90
• ACVF - AUTOMATED MANUFACTURING METHODS	133,700	0.67
• ACVF - EXISTING MANUFACTURING METHODS BASED ON ACTUALS	175,400	0.88

The cost reductions compared to the metal fin using both existing and automated manufacturing techniques indicate the ACVF is cost competitive with metal. Automation of composites compared to existing manufacturing techniques indicate a cost reduction of 25 percent. The ACVF cost, based on actuals, is 12 percent under the metal fin. Facilities and equipment requirement for the automated manufacturing techniques are estimated to be approximately \$12.1 million in 1983 dollars.

Final Cost Analysis

A final cost analysis was prepared incorporating all of the approved producibility cost reduction items updating the cost estimates based on actuals, and refining the time standards, projections, and other cost criteria. The major component costs for the metal fin and the ACVF projections for existing and automated techniques are shown in table V. Cost comparisons based on ACVF actuals to the metal fin and ACVF projected costs are also shown.

TABLE V. - COST COMPARISON BY COMPONENT (CUMULATIVE AVERAGE - 100 UNITS)

	METAL FIN	PROJECTED BASED ON EXISTING METHODS	PROJECTED BASED ON AUTOMATED METHODS	ACTUALS BASED ON EXISTING METHODS
COVERS	\$ 66,000	\$ 66,200	\$ 42,500	\$ 71,500
RIBS	40,200	28,800	19,400	24,500
SPARS	33,800	47,000	35,400	43,000
FINAL ASSEMBLY	53,300	31,400	31,400	31,400
COMMON ITEMS	5,000	5,000	5,000	5,000
	\$198,300	\$178,400	\$133,700	\$175,400
RATIO	1.0	0.90	0.67	0.88

FULL-SCALE GROUND TESTS

The ground test program consisted of a series of tests to verify the structural integrity, damage tolerance and fail safety of the composite fin box. The plan was to perform all testing on one article.

A static test would be performed first. This consisted of loading the fin box to design ultimate load including a factor to account for environmental effects.

Following static testing impact damage would be inflicted in critical locations on the cover and spar to simulate manufacturing or service damage which might go undetected. The damage would be such as to be barely visible on the outside surface. Damage would be monitored at normal service inspection intervals for one lifetime (36,000 flights) of cyclic fatigue loading.

At the completion of one lifetime, major damage would be inflicted to one cover to simulate lightning strike damage and a full cycle of design limit load including an environmental factor would be applied.

The major damage would then be repaired using in-service repair techniques and a second lifetime of cyclic fatigue loading applied.

The fin box would then be tested to destruction.

Ground Test Setup and Loads

The fin and transition structure were attached to the load reaction frame in a horizontal attitude as shown in figure 27.

The purpose of the transition structure installed between the fin box and the reaction frame was twofold. Firstly, the fin-to-transition structure interface joint duplicated the actual joint mating the composite fin to the L-1011 aircraft. Secondly, the transition structure induced the appropriate distribution of load within the fin as externally applied test loads were transmitted out of the fin and into the reaction frame. The transition structure was attached to the reaction fixture with "bathtub" type fittings, which were installed around the periphery of the base.

Externally applied side loads were introduced to the fin along the length of the front and rear spars from jack-trains which were mounted on the floor. Fore- and aft-direction external loads were applied to the fin through the rudder actuator retention brackets.

The ground test article (GTA) was tested with static loads simulating a high bending dynamic lateral gust condition. This condition was critical for the front spar and covers and adequately loaded the whole structure. A comparison of the design and test bending moments is shown in figure 28. A factor of 1.06 was applied to the loading to account for environmental effects as the tests were conducted at ambient temperature and moisture levels.

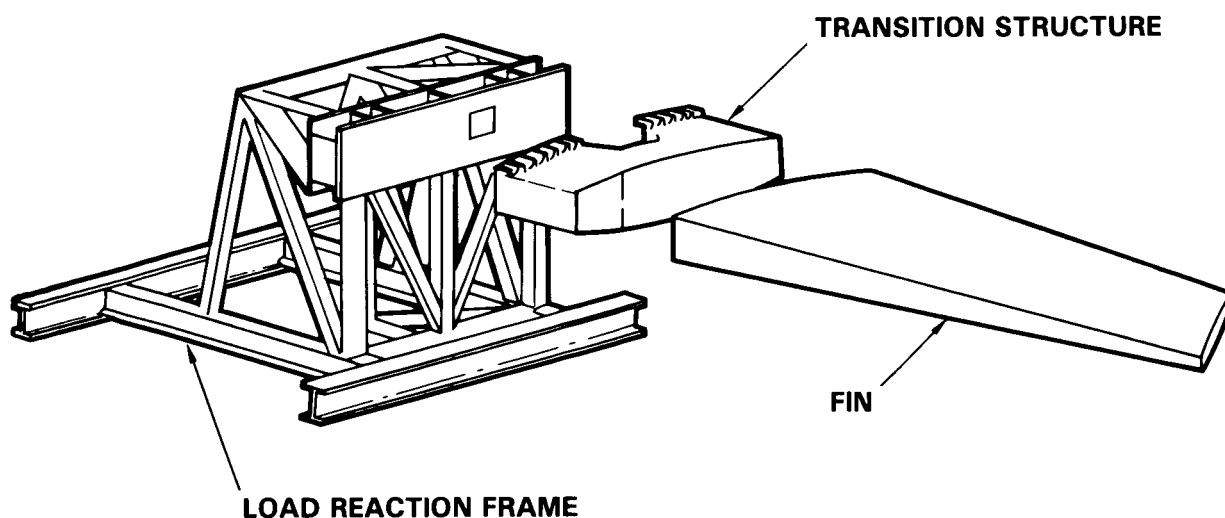


Figure 27. - Test installation of fin in load reaction frame.

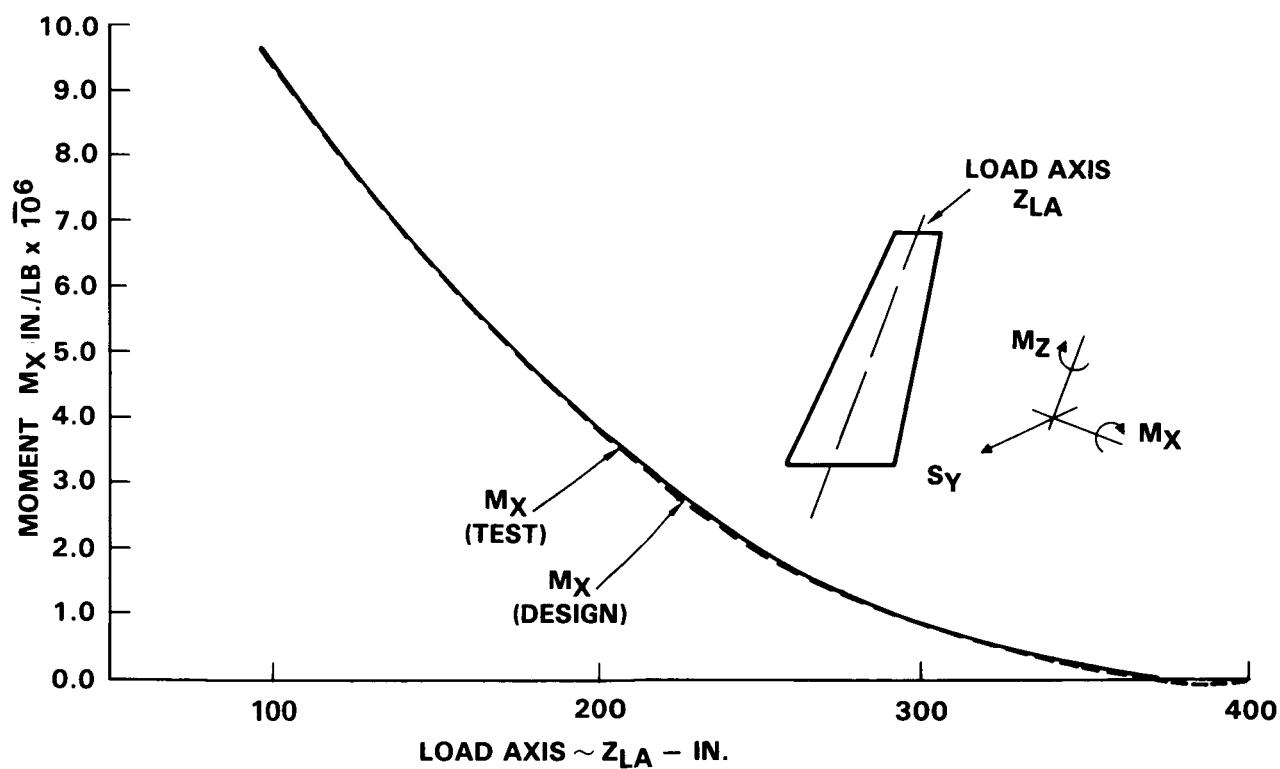


Figure 28. - Test bending moment compared with design bending moment.

The first static test resulted in an unexpected failure at 98 percent Design Ultimate Load (DUL). Following an investigation into the cause of the failure, a second ACVF (GTA No. 2) was reinforced and the test program continued. The following is an account of the failure analysis of GTA No. 1, reinforcement of GTA No. 2 and the subsequent testing of GTA No. 2.

Ground test article No. 1 - Test History.- The events leading up to the premature failure were as follows. After conducting strain surveys the fin box was loaded to Design Limit Load (DLL). A review of selected quick-look data channels showed that the fin box was performing as predicted. While the data were being reviewed the loading was reduced to 10 percent DUL and held. This was standard procedure throughout the test.

The test loading was next increased to 80 percent DUL at which point loud popping and cracking sounds were heard. The load was reduced and a visual inspection performed. It was found that some blind fasteners (MS 21140-06) in the left hand spar cap-to-cover joint had tipped. The use of blind fasteners was restricted by the fin assembly drawing to a portion of the left hand cover-to-solid web rib cap connection. The reason for installation of blind fasteners in the upper portions of the front and rear spar cap-to-cover connection above VSS 222 on the left hand side was stated on a discrepancy report to be mechanic error. No corrective action was taken to remove these fasteners as their strength was judged to be sufficient to provide a positive margin in this location. Because of the tipping, the blind fasteners in the front spar and 78 of the more highly loaded blind fasteners in the rear spar were removed and replaced with 1/4 in. or 3/16 in. oversize Hi-Loks. The heads on the 1/4 in. Hi-Loks were shaved for 0.08 countersink depth, the same as the 3/16 in. diameter.

The testing was resumed after completion of the fastener replacement. After completion of the system checkout, the load level was raised to 10 percent of DUL. The applied loads were checked to ensure that the system was operating properly. The load level was then increased to DLL and the quick-look data channels were reviewed and checked against predicted and previous test strains. This check showed that the box was behaving as anticipated. A visual examination of the exterior surface showed no damage.

The load level was then raised to 90 percent DUL. Some creaking noises were heard between 80 and 90 percent. Strain measurements compared well with anticipated results. The load level was next raised toward the goal of 106 percent DUL. At 98 percent DUL failure occurred.

Ground test article No. 1 - Failure Analysis.- The failure resulted in damage to the front spar left-hand cap from root to tip, local left-hand cover damage including separation of the skin and stiffener in the run-out bays toward the tip, separation of rib to front spar web attach members at all rib stations, and left-hand rib cap damage on most of the truss ribs along the line of a skin buckle between cover stiffeners 8 and 9. The left-hand cover was the tension surface in this test.

Examination of movie film taken during the test indicated that failure initiated in the front spar cap between VSS 299.97 and VSS 323.62.

The failure sequence has been identified as follows: The spar cap failed first in interlamina tension between VSS 299.97 and VSS 323.62. The failure then progressed along the spar to the tip and then to the root. The initial failure and subsequent progression along the spar caused an increase in axial load in the free edge of the cover and high torsional deflections resulting in tearing of the cover at solid rib stations VSS 299.97 and VSS 274.25, buckling of the skin and disbonding of hat stiffeners near the front spar. Due to the open box section, the shear center shifted aft behind the rear spar and caused a large increase in the compression load in the left-hand truss rib caps resulting in progressive failure of the rib caps down to and including VSS 145.71. The rotation of the front spar cap about the right-hand surface (lower surface in test setup) caused failure of the rib connection to the spar.

The front spar cap configuration in the area of the primary failure consists of four plies of +45 degree or -45 degree orientation, then 10 plies of 0 degree orientation, and four more +45 degree or -45 degree plies. The four plies from each side of the spar web are continued around to become part of the spar cap. The remaining 12 web plies terminate at the cap. A photomicrograph (figure 29) of a section of the right-hand front spar cap in the primary failure zone shows that failure initiated in this location. The four plies of web material have separated from 0 degree cap material through the radius and into the flange. A crack extends across the web.

The spar failure was caused by out-of-plane loads which inflicted interlamina tension and bending on the spar caps. These loads come from several sources. Transverse cover loads were due primarily to Poissons effects and these were offset from the spar cap mid plane, thus introducing bending. Shear buckling of the trapezoidal panels adjacent to the front spar cap introduced both bending and normal loads to the spar cap plus diagonal tension loads. A load also resulted from the spars pulling down the upper cover to conform with the deflected shape. The cover curvature due to airfoil camber also introduced a normal component of load. Some of the loads are additive and some subtract, and the net effects varied with the location.

As a result of the ground test some redesign would be necessary before the fin could be committed to production. A redesign of the spar would include taking all the web plies around into the cap, and the cap would be designed for specified out-of-plane loading. Figure 30 shows a schematic of the original cap and the redesigned cap. It is estimated that a redesign of the spars would add about 15 lbs. This would be due to thicker spar caps when all the web plies are continued into the cap flanges, the elimination of the lower six access holes in the front spar web and the replacement of the front

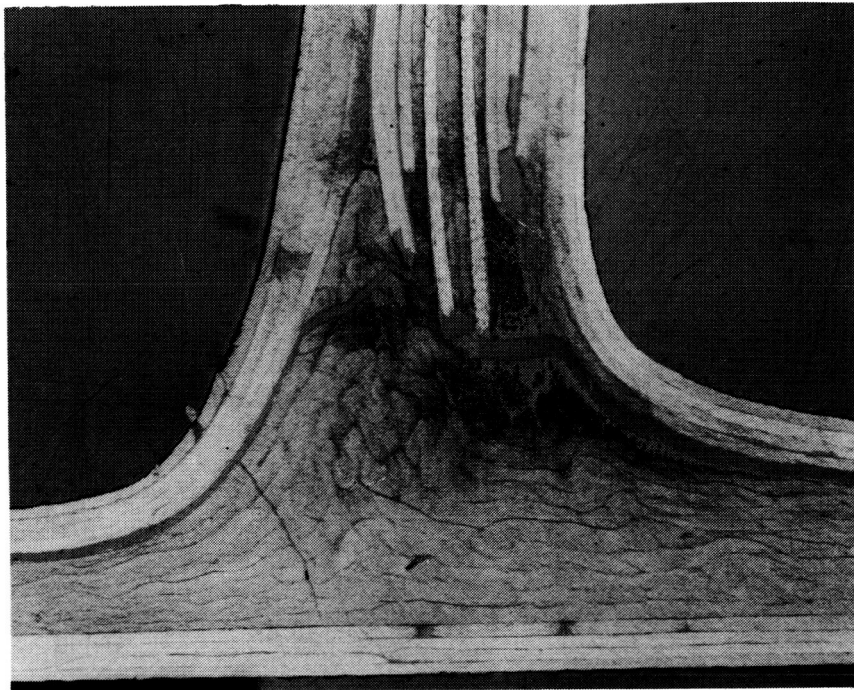


Figure 29. - Photomicrograph of section from GTA No. 1 front spar cap, right side at VSS 278.3.

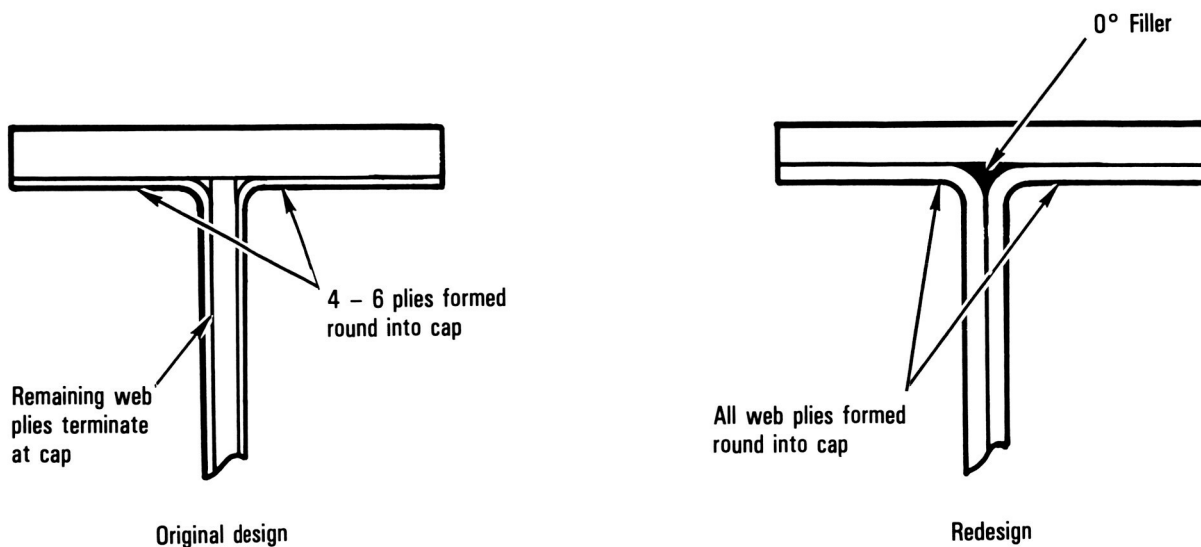


Figure 30. - Schematic of original spar cap and redesigned spar cap.

spar web to rib cocured graphite/epoxy tees with mechanically attached aluminum angles. The covers would also increase in weight by about 5 lb because of an increase in the thickness of the skin in the stiffener runout bays and the addition of some mechanical fasteners. This will reduce the weight saving from 27.4% to 25.2% (216 lb). A comparison of the redesigned composite fin to the aluminum fin is shown in table VI.

Ground test article No. 2.- It was decided to perform a "production line" fix on the second ACVF to preclude the types of failures encountered with GTA No. 1. The failure investigation on GTA No. 1 showed that the front spar caps failed, the rib to front spar web attachment angles debonded from the spar web and the cover hat stiffeners adjacent to the front spar in the outboard bays debonded.

In order to provide more strength to resist out-of-plane loads, the existing spar caps were reinforced with formed aluminum angles from root to tip. Figure 31 shows the configuration of the angles which are 0.063 in. thick 2024-T3 material. The angles were installed in short lengths (approximately 3 in.) to minimize their picking up axial load.

The ribs are attached to the front spar web through a cocured graphite/epoxy tee. At the rear spar the ribs are attached through aluminum angles which are located and mechanically attached on assembly. A secondary failure on GTA No. 1 involved the separation of the cocured graphite/epoxy tee on the front spar. These tees were reinforced with aluminum angles as shown in figure 32. The angles are 0.063 in. thick 2024-T3 mechanically attached to the web.

The trapezoidal skin panels adjacent to the front spar in the 10-ply skin area above VSS 248 buckled in shear below limit load. During the failure sequence on GTA No. 1 the stiffeners adjacent to the front spar debonded primarily along the forward flanges in the 10-ply area. The skin was too thin to countersink for fasteners to preclude the debonding of the skin and stiffener in the run-out bays. For GTA No. 2, 0.032 in. aluminum doublers were bonded and mechanically attached to the left and right hand covers locally, as shown in figure 33. These doublers were dimpled at the front spar cap to fit the

TABLE VI. - COMPARISON OF METAL FIN TO COMPOSITE FIN

	Metal Box	Composite Box
Weight (lb)	858	642
Percent Composite Material	-	76
Weight Saved (lb)	-	216
No. of Ribs	17	11
No. of Parts	716	201
No. of Fasteners	40,371	6,911

existing countersinks. The doublers also were countersunk, for the 5/32 in. diameter HL11 fasteners installed along the stiffener flanges.

The addition of this reinforcement added 42 lb to the fin which reduces the weight saving to 22.5 percent. In a composite redesign, 20 lb instead of 42 lb would be added for a total weight savings of 25.2 percent.

The test setup and the applied loads for GTA No. 2 were identical to those for GTA No. 1. Some changes were made in strain gage locations based on the results from GTA No. 1.

Static test.— Prior to static testing, a strain survey to 50 percent DUL was performed. The fin box was found to be responding as anticipated. Static tests were all performed with jacks pulling down so the right-hand surface was in compression and the left-hand surface was in tension. For damage tolerance and fail-safe testing, all loading was fully reversed so both surfaces saw the same tension and compression loading.

Testing commenced by loading to Design Limit Load. Data from selected key strain gages were reviewed to establish that the fin box was behaving as anticipated. The fin box was then loaded to 106 percent DUL and then back to zero. The extra 6 percent DUL was to cover the estimated environmental degradation effects as discussed previously.

At 106 percent DUL, the maximum cover axial strain was about 2800 in/in. with local strains in a buckled area at about 4000 in/in. The right-hand cover 16-ply skin between VSS 121 and VSS 97 near the rear spar buckled in compression at 82 percent DUL, which was consistent with the PRVT static cover tests where buckling initiated between 78 and 108 percent DUL under uniaxial loading. The trapezoidal cover panels in the lower 14-ply bay adjacent to the front spar were instrumented with back-to-back shear rosettes. Buckling occurred on both tension and compression covers.

There was no evidence of any buckling on the spar webs. Shear strains in the front spar webs were fairly even, ranging from 3600 in/in. to 4600 in/in. The rear spar shear strains were low, with a maximum of 1600 in/in. A post-test inspection revealed no damage or loose fasteners.

Damage Tolerance Testing

Once the static testing was completed GTA No. 2 was prepared for the damage tolerance testing. The load cells and jacks required changing for the damage tolerance test because of the lower loads applied during the cyclic tests, and because the loads were fully reversed through tension and compression. The load cells thus required a greater sensitivity and the jacks a longer stroke.

The fatigue spectrum employed contained 197,000 cycles representing the 36,000 flight lifetime. The loads were applied as fully reversed load cycles. This fatigue spectrum is a little more severe than applied to the L-1011 fatigue test article. The final flight loads included the application of design limit load with a 1.06 environmental factor.

The fin box was impacted, for the damage tolerance evaluation, at the locations shown on figure 34. Impacting was performed using a calibrated impactor gun. The impactor was a 1 in. diameter steel ball. The initial impact energy levels were determined from trials on ancillary test components of similar configuration. All cover impacts were over stiffener flanges in the most critical areas for each skin thickness.

Impact No. 1 was in the 16-ply skin area near the aft region of the cover root end. One impact at 13.33 ft-lb was sufficient to cause visible surface damage.

Impact No. 2 was in the 14-ply skin area. Four impacts were required to obtain visible damage. The first impact was at 13.33 ft-lb. Some damage was evident ultrasonically. A second impact at 8.64 ft-lb showed no evidence of change ultrasonically. A third impact, now back at 13.33 ft-lb, gave no visible damage but increased the damage area determined ultrasonically. A fourth impact was made, but at an energy level of 18.95 ft-lb. Visible penetration through the thickness occurred.

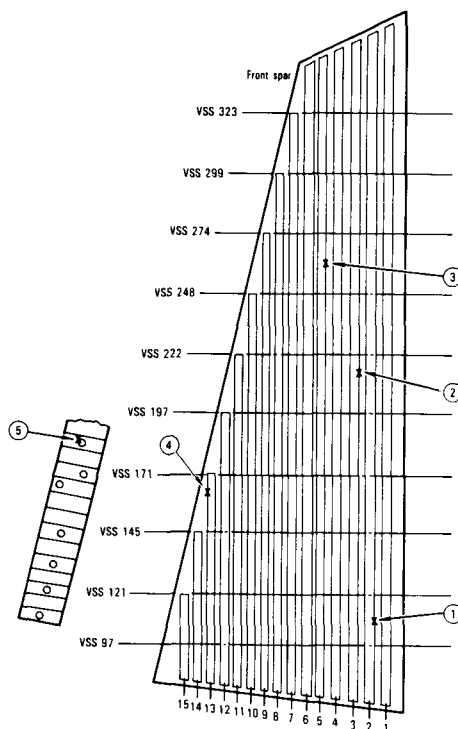


Figure 34. - Impact damage locations.

Impact No. 3 was in the 10-ply skin area. This area was impacted at 13.33 ft-lb also. One impact caused visible surface damage.

Impact No. 4 was in the 16-ply skin area adjacent to the front spar. Because this area was very rigid it was anticipated that lower impact levels would cause damage. However after six impacts at 8.64 ft-lb no visible damage occurred internally or externally, and the ultrasonically determined damage area remained essentially unchanged after the first impact. Two more impacts at the higher energy level of 13.33 ft-lb again made little difference. There was some evidence of hat flange skin separation extending to the rib about 3 inches away. It was decided to do no more impacting in this area.

Impact No. 5 was on the front spar web at the lowermost unreinforced access hole. The first impact at 7.99 ft-lb gave no visible damage. A second impact at 12.52 ft-lb gave visible delamination of the surface and in the edge of the access hole.

At the completion of each one-quarter lifetime (9000 flights) of fatigue loading the impacted areas were inspected ultrasonically and damage growth, if any, marked on the part. The damage and growth for impact No. 2 shown in figure 35 is typical of that which occurred at all five locations. Most growth occurred during the first half lifetime of fatigue cycling and could only be determined ultrasonically.

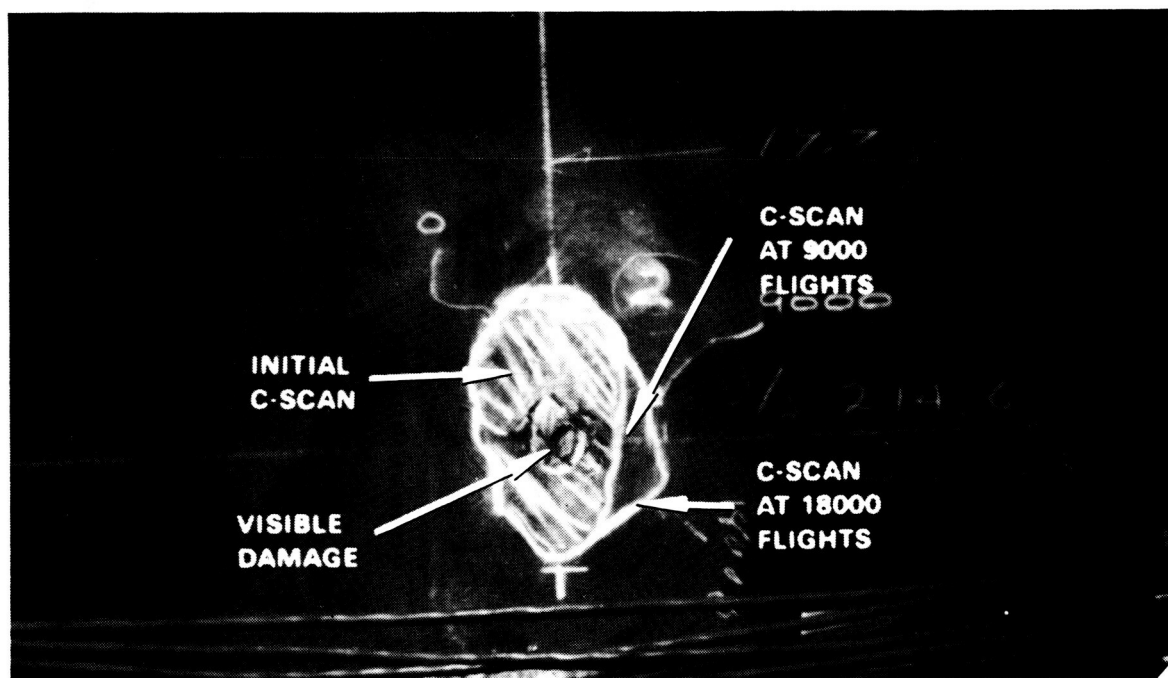


Figure 35. - Impact No. 2 damage growth.

Discrete Damage Test and Repair

At the completion of one lifetime, simulated lightning strike damage was inflicted to the fin cover. The area selected was considered to be the most critical for large area damage. An area on the left-hand cover between VSS 97.19 and VSS 121.1, approximately 12 by 4 in. and at a 45-degree angle to the rear spar, was damaged by impacting to obtain delaminations. A hole was then burned through the skin using an electric arc from a 3/16 in. diameter welding rod. The delaminated area was then burned with oxygen/acetylene flame torch to char the outer plies. The resulting overall damage is shown in figure 36.

The fin box was then loaded to 1.06 design limit load in both directions, so the damaged cover was loaded once in tension and once in compression. A post test ultrasonic inspection showed no growth in any of the damage.

The discrete source damage was then cleaned up and repaired. A schematic of the repair is shown in figure 37. Visual inspection of the completed repair showed no discrepancies. Ultrasonic inspection of the patch indicated distributed porosity in the adhesive. The porosity had been anticipated based on previous patch tests and was acceptable. The repair technique was based on a method developed under another NASA Langley Research Center contract with Lockheed, NAS1-15269, entitled "Development, Demonstration, and Verification of Repair Techniques and Processes for Graphite/Epoxy Structures for Commercial Transport Aircraft" (reference 7).

A second lifetime of damage tolerance testing followed. On completion of this second lifetime of fatigue cycling an ultrasonic inspection revealed no change in any of the damage areas and no effect on the repair.

Residual Static Strength Test

The fin box was statically tested to determine its residual strength. Failure was expected to occur at approximately 120 percent DUL. Failure occurred at 119.7 percent DUL in the left-hand (tension) cover near the front spar and between the rib at VSS 222 and that at VSS 248. The high speed movies indicated that failure initiated just above the VSS 222 rib when the cover skin and the forward cover stiffener separated. Failure propagated outboard to VSS 248 and inboard to VSS 145.

Figure 38 shows the fin box as failure occurred. The buckle in the cover skin shows the extent of the skin stiffener separation. Rib cap failures occurred in line with the buckle from VSS 222 to VSS 145.

The initial failure was caused by high interlaminar stresses induced by shear buckling of the trapezoidal skin panel between VSS 222 and VSS 248 and between the front spar and stiffener No. 10. The high speed film showed that the skin buckled up just above VSS 222 and the buckle then propagated outboard and inboard as the skin and stiffener separated. Shear buckling was measured by a pair of back-to-back shear rosettes in the bay below VSS 222. The strain gage plots shown in figure 39 indicate that shear buckling initiated at about

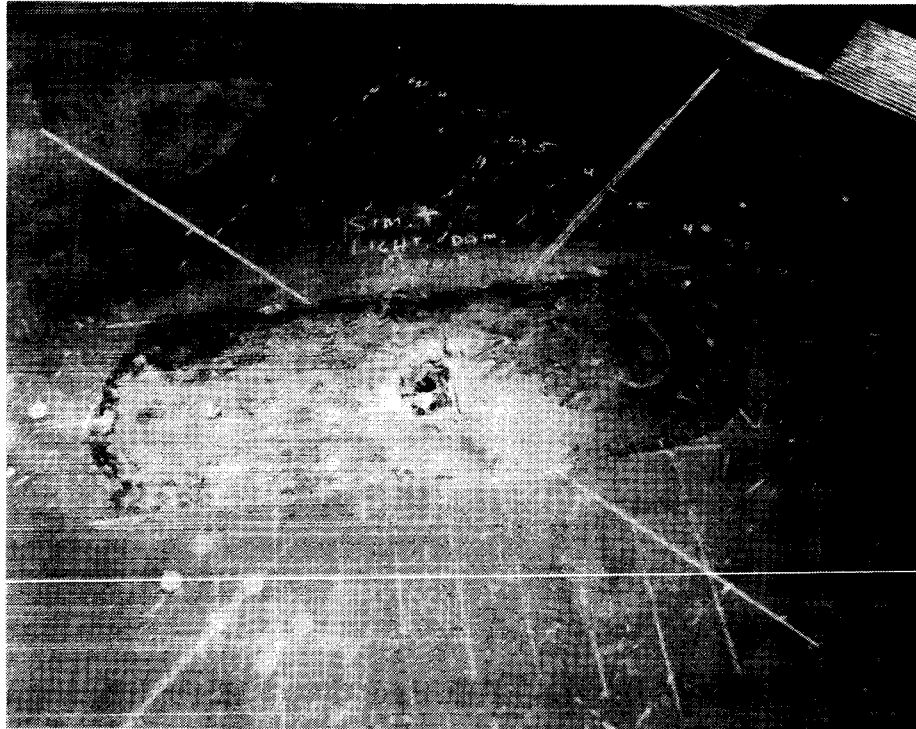


Figure 36. - Simulated lightning damage.

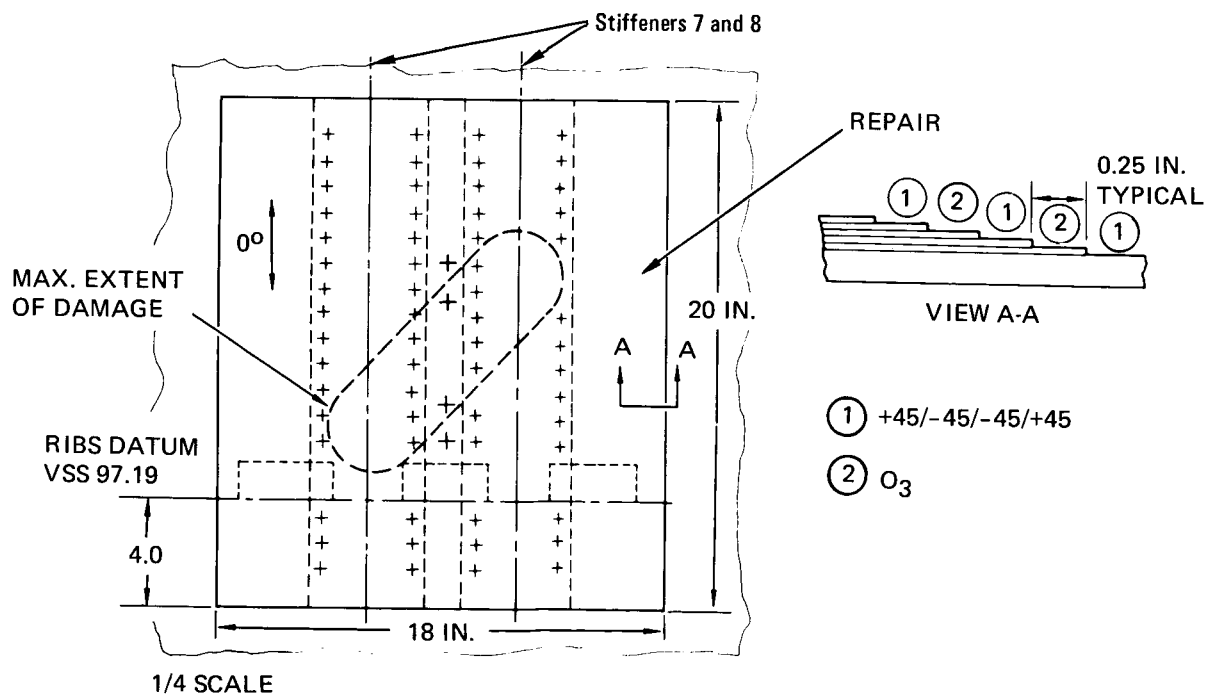


Figure 37. - Damage repair.

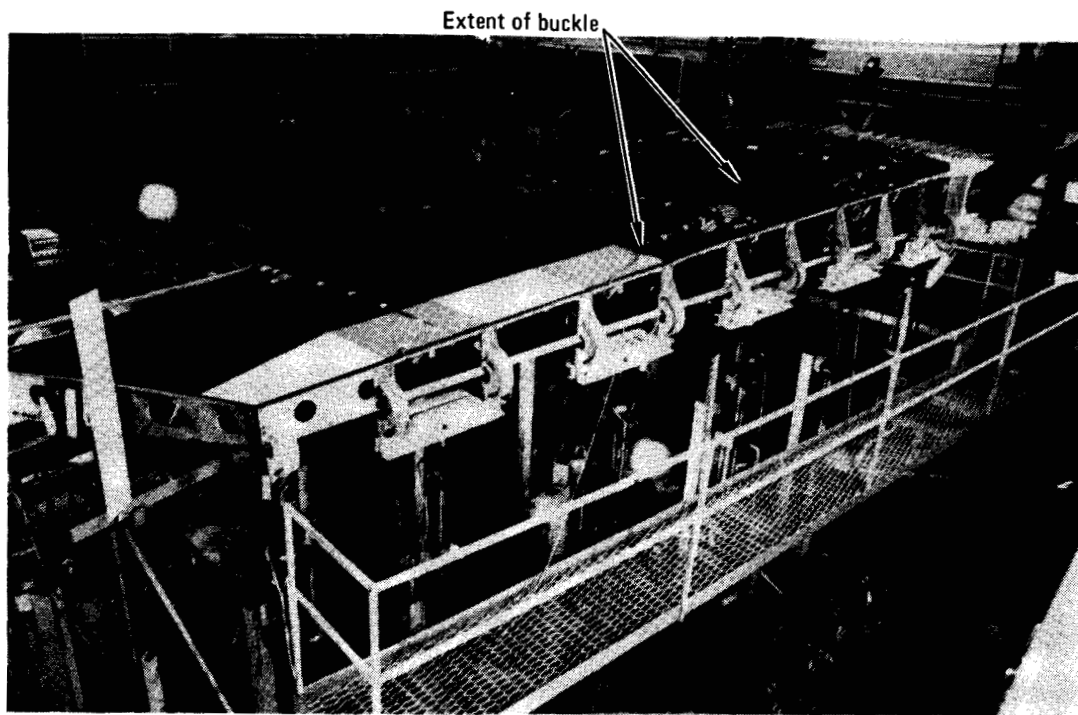


Figure 38. - Fin box at the moment of failure.

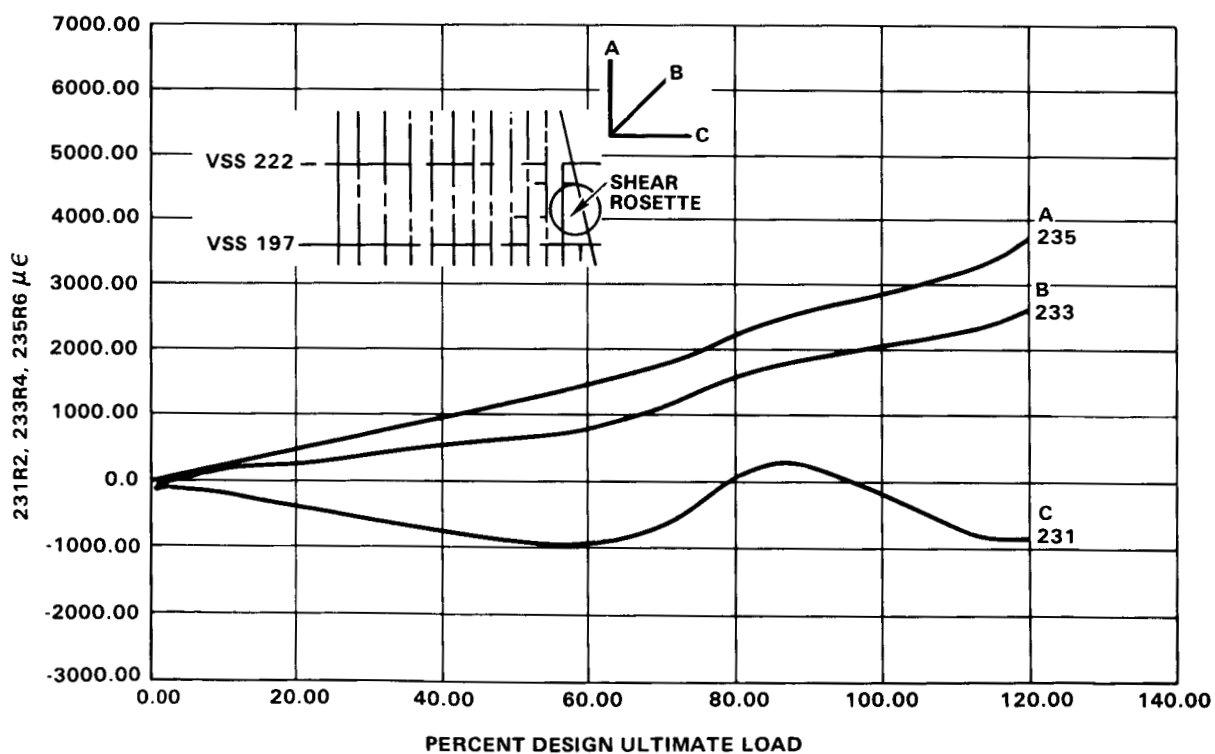


Figure 39. - Shear rosette strain gage plots on tension cover in bay below the failure bay.

design limit load. The Poisson-induced lateral compression strain combined with the shear caused the initial buckling and proved to be more severe than the axial compression and shear on the other cover which did not buckle until 80 percent DUL.

The strains at 106 percent DUL compared very well with those from the static test performed on this GTA on April 7, 1982, even in the locations where the strains were nonlinear due to buckling. This indicates that no degradation occurred during the damage tolerance tests. The failures were very similar to those which occurred on GTA No. 1. The spar cap and rib-to-spar web reinforcement prevented failures in those locations and the cover doublers moved the failure initiation bay down to the first bay without a doubler. The conclusion is that the failure in both GTA No. 1 and GTA No. 2 was due to interlaminar tension loading caused by shear buckling of the cover skin panel between the front spar cap and the adjacent hat stiffener. In GTA No. 1 the failure apparently initiated in the spar cap, and in GTA No. 2 failure initiated at the skin-to-stiffener interface near VSS 222.

Lessons Learned

Small out-of-plane loads cannot be ignored in composite structures. Flanges on such structures as spars, covers, frames and ribs must be designed to withstand out-of-plane loads.

CONCLUSIONS

The results obtained in this program show that advanced composites can economically and effectively be used in the design and construction of medium primary structures for commercial aircraft.

Static strength variability has been demonstrated to be comparable to metallic structures. The range of production qualities has been established. The long-term durability of advanced composite components has been demonstrated.


Advanced composites have been shown to be cost competitive and production fabrication techniques have been demonstrated.

The importance in composite structures of accounting for the effects of small out-of-plane loads usually ignored in the design of metal structures has been identified.

The damage tolerance and fail-safety of the design was verified by full-scale ground tests and an in-service repair technique was verified.

REFERENCES

1. Ary, A., et al, Flight Service Evaluation of an Advanced Composite Empennage Component on Commercial Transport Aircraft, Phase I Final Report, Engineering Development, NASA CR-144986, May 1976.
2. Jackson, A. C., et al, Advanced Manufacturing Development of a Composite Empennage Component for L-1011 Aircraft, Phase II Final Report, Design and Analysis, NASA CR-165634, April 1981.
3. Jackson, A.C., et al, Advanced Manufacturing Development of a Composite Empennage Component for L-1011 Aircraft, Phase III Final Report, Production Readiness Verification Testing, NASA CR-172383, 1984.
4. Alva, F., et al, Advanced Manufacturing Development of a Composite Empennage Component for L-1011 Aircraft, Phase IV Final Report, Manufacturing Development, NASA CR-165885, May 1982.
5. Jackson, A., Dorward, F., Advanced Manufacturing Development of a Composite Empennage Component for L-1011 Aircraft, Phase V Final Report, Full-Scale Ground Test, NASA CR-166015, December 1982.
6. James, A.M., and Bohon, H.L., Production Readiness Verification Testing, Proceedings of the Third International Conference on composite Materials, Paris, France, August 1980.
7. Stone, R. H., Repair Techniques for Graphite/Epoxy Structures for Commercial Transport Applications, NASA CR-159056, January 1983.

1. Report No. NASA CR-3816		2. Government Accession No.		3. Recipient's Catalog No.	
4. Title and Subtitle ADVANCED COMPOSITE VERTICAL FIN FOR L-1011 AIRCRAFT - DESIGN, MANUFACTURE, AND TEST (EXECUTIVE SUMMARY)				5. Report Date September 1984	
				6. Performing Organization Code	
7. Author(s) A. C. Jackson				8. Performing Organization Report No. LR 30736	
9. Performing Organization Name and Address Lockheed-California Company P.O. Box 551 Burbank, California 91520				10. Work Unit No.	
				11. Contract or Grant No. NAS1-14000	
12. Sponsoring Agency Name and Address National Aeronautics and Space Administration Washington, DC 20546				13. Type of Report and Period Covered Contractor Report	
				14. Sponsoring Agency Code	
15. Supplementary Notes Langley Technical Monitor: Marvin Dow					
16. Abstract The structural box of the L-1011 vertical fin, was redesigned using advanced composite materials. The box was fabricated and ground tested to verify the structural integrity. This report summarizes the complete program starting with the design and analysis and proceeds through the process development ancillary test program production readiness verification testing, fabrication of the full-scale fin boxes and the full-scale ground testing. The program showed that advanced composites can economically and effectively be used in the design and fabrication of medium primary structures for commercial aircraft. Static strength variability was demonstrated to be comparable to metal structures and the long term durability of advanced composite components was demonstrated.					
17. Key Words (Suggested by Author(s)) Composites Transport aircraft Primary structure Graphite epoxy Design testing Manufacture				18. Distribution Statement  Subject Category 24	
19. Security Classif. (of this report) Unclassified		20. Security Classif. (of this page) Unclassified		21. No. of Pages 61	
				22. Price	